INVESTIGATION OF A PASSIVE, TEMPORAL, NEUTRON MONITORING SYSTEM THAT FUNCTIONS WITHIN THE CONFINES OF START I

THESIS

Stephanie Vaughn
Major, USA

AFIT/GNE/ENP/03-10

DEPARTMENT OF THE AIR FORCE
AIR UNIVERSITY

AIR FORCE INSTITUTE OF TECHNOLOGY

Wright-Patterson Air Force Base, Ohio

AFIT/GNE/ENP/03-10

INVESTIGATION OF A PASSIVE, TEMPORAL, NEUTRON MONITORING SYSTEM THAT FUNCTIONS WITHIN THE CONFINES OF START I

THESIS

Presented to the Faculty

Department of Engineering Physics

Graduate School of Engineering Management

Air Force Institute of Technology

Air University

Air Education and Training Command

in Partial Fulfillment of the Requirements for the

Degree of Master of Science (Nuclear Science)

Stephanie Vaughn, BS

Major, USA

March 2003

AFIT/GNE/ENP/03-10

INVESTIGATION OF A PASSIVE, TEMPORAL, NEUTRON MONITORING SYSTEM THAT FUNCTIONS WITHIN THE CONFINES OF START I

Stephanie Vaughn, BS
Major, USA

Approved:

James C. Petrosky (Chairman)	6 MAR 03 date
Larry W. Burggraf (Member)	6 Mar 2003 date
George John (Member)	6 Mar 2003 date

Acknowledgments

I would like to thank my husband and my son for their patience and support during this period. The family time sacrificed during the course of this research cannot be repaid but was directly responsible for my success in this endeavor. You were both the rock I leaned on and the light at the end of my tunnel.

I would like to express my sincere appreciation to my faculty advisor, LTC James C. Petrosky, for his guidance and support throughout the course of this effort. The insight and experience was unquestionably valued. I would like to thank the other distinguished members of my committee, Dr. Larry W. Burggraf and Dr. George John, their interest was appreciated and their expertise was invaluable.

I would also like to thank laboratory technician, Mr. Eric Taylor, whose assistance, skill, and knowledge were imperative to the success of this project. Mr. Russ Hastings and the other members of the AFIT machine shop are forever in my gratitude. Their willingness to provide assistance and the equipment they fabricated was key to the completion of this project.

Stephanie Vaughn

Table of Contents

List of Figures

List of Tables

Abstract

This study is an investigation of the theoretical and experimental possibilities of using activation foils to detect and monitor special nuclear material for treaty monitoring purposes. None of the experiments demonstrated sufficient sensitivity to detect the target flux of 0.5 neutrons/cm^2-sec. The target flux could be detectable, if the limit of detection had been reduced by a factor of 4 to 6. However, many issues identified could enhance the sensitivity including: increasing foil size, increasing detector efficiency, and optimizing foil selection.

The theoretical portion focused on gold, silver, indium, europium, and gadolinium foils and determined the minimum flux detectable, minimum time needed to detect a specific flux, and what gaps in coverage exist when a detection package consists of all combined foils. All calculations are based on actual gamma and beta detector responses and statistics in a high and low background.

The second section consists of experiments with gold, indium, and silver foils. Detectors in a low background counted emitted gammas or betas to establish three-sigma limits of detection, which is the lowest neutron flux detectable with a 99 percent statistical reliability. The dominant factor in determining the limit of detection is the error associated with the total activity. The determined value for limit of detection was used to calculate the minimum foil surface area required to detect the target flux.

INVESTIGATION OF A PASSIVE, TEMPORAL, NEUTRON MONITORING SYSTEM THAT FUNCTIONS WITHIN THE CONFINES OF START I

I. Introduction

Background

The future of arms control is unclear and the threat of terrorism reinforces the need to account for all nuclear materials. With the signing of the Moscow Treaty and the war on terrorism there may be a greater need for multilateral treaties to obtain positive control of special nuclear materials (SNM) and weapons. This thesis defines SNM as weapon-grade plutonium (WgPu) and weapon-grade uranium (WgU).

While arms control's future form is unknown, the direction is clearly given in the Strategic Offensive Reductions Treaty's Text of Joint Declaration.

> The United States and Russia recognize the profound importance of preventing the spread of materials and technology that could be developed into weapons of mass destruction and missiles. The specter that such weapons could fall into the hands of terrorists and rogue states who support them illustrates the priority all nations must give to combating proliferation. (1)

On May 24th, 2002, President Bush and Russian President Putin signed the Strategic Offensive Reduction Treaty, also known as the Moscow Treaty. If ratified by the United States Congress and the Russian Duma, the Moscow Treaty will mandate the reduction of both Russian and American deployed nuclear weapons by almost two-thirds, from the Strategic Arms Reduction Treaty of 1991 (START I) levels of 6,000 to between 1,700 and 2,200 by December 31, 2012. The Moscow Treaty compliments the existing in-place procedures of START I. The Bush White House Press Secretary stated "START I's comprehensive verification regime would provide the foundation for transparency and predictability regarding implementation of the new bilateral Treaty." (2)

The arms control treaties between the United States and Russia require that both parties be confident the other is complying with the terms of the current treaty. These conditions create the requirement for accurate systems to detect and verify the presence of SNM. Reliable and easy to understand systems for detecting the signatures of SNM develop confidence in the strategic arms control process.

Problem

Nuclear weapon verification inspections resulted from the arms reduction efforts between both the United States and Russia. START I and the Moscow Treaty provide the authority for each country to inspect the other country in order to verify compliance with the treaties. Limitations on the procedures for weapon verification are in place to maintain the secrecy of weapon design and prevent the transfer of classified or restricted information. The signatories have agreed not to open warheads or containers to physically observe the presence of the nuclear weapon and only use passive and non-imaging detectors.(3) As a result of these limitations, detectors need to identify SNM of unknown size and shape contained within an unknown surrounding material.

Nuclear weapons and their components in storage containers are large, dense, and nonhomogenous. Signatures must penetrate far enough to escape from the interior of the weapon or container and reach a detector. Signatures must possess sufficient intensity to complete an inspection measurement in the time allowed. The inspector has only 10 to 15 minutes per weapon to make a detector reading, which inhibits the use of conventional detection methods. (4)

As more countries with smaller-scale nuclear weapons programs evolve, more weapons should fall under arms control agreements. To deter proliferation and for treaty verification purposes, a system that accurately detects extremely low levels of nuclear isotopes is needed for weapon accountability, specifically for confirming the continuous

presence of a weapon or weapon components in a container.(4) To limit the transfer of weapon design information, passive detection, the detection of the radiation emitted by radioactive decay, is the only allowable method for treaty verification and accountability purposes. Neutrons are of particular interest because they are indicators of spontaneously fissioning material. Due to their neutral nature, neutrons can escape from the interior of nuclear weapons and their containers to be detected.

Arms control inspectors face many problems when trying to establish a chain-of-custody for SNM. Treaties permit inspectors only short, periodic visits. The chain-of-custody of each storage container can only be demonstrated with a system of security seals and tags or by a highly involved computer monitoring system that may not follow a container throughout its lifetime.

The dismantlement phase causes particular problems with the chain-of-custody in the weapons life cycle. (5) Even though control tags and seals are compromised, inspectors are not allowed to observe any phase of dismantlement including: the removal of the warhead from its container, the dismantlement process, and the components placed in component containers. Access is denied because of national security interests and the possibility of revealing critical information. Because of this, it is not possible to maintain physical, hands-on, custody of every weapon within this system. Therefore, the United States needs to develop methods to verify that what enters at one end of the process actually exits at the opposite end.

Before and after the weapon dismantlement process, the containers holding SNM will possibly undergo transport to a storage facility for long-term storage. Treaties require periodic inspections to determine whether the storage containers have been tampered with in a manner violating arms control agreements. One aspect to determine if tampering takes place is to determine if the SNM has remained inside the container for the entire

monitoring period. An ideal monitoring system is reliable, tamper proof, low cost, low maintenance, and could be measured onsite.

To overcome the difficulties in monitoring SNM, DTRA has begun researching potential monitoring systems to maintain a chain-of-custody. DTRA needs detection devices to verify that what is claimed to be within the container is truly in the container, especially when the chain-of-custody has been lost. Finally, DTRA needs a more comprehensive "cradle-to-grave" system of monitoring storage containers holding nuclear weapons or components in all life cycle stages. (5) A technology that can show a component to have been in a container continuously for a period of time consistent with declared activities can provide confidence that accountability of all SNM has been maintained.

A Possible Solution

A possible solution for maintaining the chain-of-custody for all SNM is a neutron activation foil detector system, attached to the outside of a storage container that constantly and passively detects the neutron flux. A neutron activation foil detector system offers unique advantages for use during long-term storage, shipping, and weapons dismantlement phases of nuclear weapons arms control. A neutron detector attached to the container significantly increases the difficulty of diversion and subterfuge. Because they are neutral, neutrons are quite penetrating and can be detected outside of most containers. An activated neutron foil system may independently confirm the item inside the container is a neutron source, provides some historic information about the neutron flux, and can help establish a more comprehensive chain-of-custody. After a period of exposure, an inspector can remove the neutron activation foil detector system and measure the activity. Over the course of several inspections and years, inspectors would

attach new neutron activation foils to storage containers to replace foils removed during inspection.

Single isotope activation foils are integrating detectors and can provide no information about time variation of the neutron flux over the course of the exposure. However, if foils of different materials are used together and compared with theoretical models, the measured activity may be used to determine if the neutron source has been tampered with. Within 8 hours, short-lived activation species can be used to assess the incident flux while the activity of longer-lived activation species continue to increase based on the cross section and half-life characteristics. Neutron activation foils possess the advantages of small size, low cost, and insensitivity to gamma radiation fields. They can also tolerate exposure to extreme temperatures, shock, and magnetic fields while requiring no electrical power. Though activation foils are frequently used in nuclear reactors to map the spatial variation of steady-state neutron fluxes, this thesis describes applications in a much weaker neutron flux.

This detection/monitoring system supports the chain-of-custody concept while keeping the exchange of design information to a minimum. Chain-of-custody offers inspectors confidence in the status and location of all SNM, which increases confidence that no unauthorized tampering of the SNM has occurred.

Scope

This thesis investigated activation theory. Additionally, experiments were performed to establish baseline detection parameters. The ideal system protects design information, is portable, operates under power and logistics restrictions, is rugged, weatherproof, tamper-proof and can retain authenticated data. Finally it must be easy to understand and reliable which builds confidence in the system.

DTRA has the mission to monitor and verify treaty compliance for the United States and is the sponsoring agency for this thesis. The focus of this study is to determine the

answer to five groups of questions dealing with the ability of activation foils to detect SNM. Specifically, the questions are:

1. What is the minimum neutron flux that will produce an activity that can be detected?

2. What is the minimum activation time necessary in a particular neutron flux that will produce an activity that can be detected?

3. If foils are used together in a detector system, will they provide continuous coverage over a 700-day period?

4. What are the limits of detection for each foil investigated?

5. What is the minimum foil area required to detect the neutron flux on the outside of a storage container?

Paper Sequence

A more in-depth analysis of the problem and testing procedures is discussed in the following chapters. Chapter II describes the theory behind foil activation. Chapter III provides the testing procedures. Chapter IV contains the experimental results and analysis. Chapter V contains conclusions and recommendations for future study. Annexes A through E provide supporting calculations, tabulated data, and references used throughout the thesis.

II. THEORY

There are three sections in this chapter. The first section provides a review of the principles of neutron activation. The second section provides a review of detector characteristics for the high purity germanium detector, the Alpha/Beta detector, and the Bonner sphere. The last section discusses an unclassified thermal neutron flux on the outside of a nuclear weapon storage container and describes a PuBe neutron spectrum.

Definitions

The following definitions are used throughout this thesis.

Neutron Flux

Neutron flux is the rate of emission or transmission of neutrons that cross a planar area per energy group. This thesis focuses on thermal neutron energies and assumes the neutron flux is constant.

Gamma Spectrum

Gamma spectrum, a high-energy portion of the electromagnetic radiation spectrum, is a characteristic increase in intensity of radiation at specific energies that correspond to the gamma energy emitted as the product of radioactive decay.

Background

Background refers to the gamma or beta background during the counting of the foils. The effect of the neutron background is not investigated in this thesis.

Neutron Detection

The detection of neutrons is an important component in monitoring SNM because neutrons indicate the presence of spontaneously fissioning material, such as plutonium and uranium. The majority of energetic neutrons are produced in alpha-n reactions (α,n) and spontaneous fissions (SF). (6)

Alpha decay is the dominant decay mode for plutonium and uranium isotopes. When an alpha particle is absorbed by a low atomic number element, such as oxygen, carbon, or silicon, a neutron may be produced. The average number of neutrons per SF for energies less than 1 MeV is 2.89 for ^{239}Pu. (7) Neutrons produced by SF and (α,n) reactions cause the release of additional neutrons by two mechanisms: induced fissions in fissile material and a (n, 2n) reaction in other materials such as beryllium. (6)

Direct electrical detection of neutrons is not possible because they have mass but no electrical charge and do not directly produce ionization in a detector. (8) Neutron detectors rely upon various interactions of an incident neutron with a nucleus to produce a secondary charged particle by elastic scattering, inelastic scattering, or transmutation, which are detected by counting the charged particles. The presence of neutrons is deduced by counting the gammas and betas emitted by radionuclides produced by the transmutation.

Activation

Because neutrons are difficult to detect, activation is used to produce gamma rays and beta particles, which are proportional to the neutron flux and easier to detect. Activation is the conversion of a stable isotope into a radionuclide by the absorption of a neutron. In order to conserve energy, energy is released in the form of radiation whose energy and frequency are determined by the decay scheme of the individual isotope.

Mechanics

The rate of activation for neutron interactions, R, in a volume, V, is given by the neutron flux, ϕ, times the total macroscopic activation cross-section, Σ_{act}, (8) or

$$R = \phi \Sigma_{act} V \ . \qquad [1]$$

The relationship (9),

$$\Sigma = N_T \sigma_{act} , \qquad [2]$$

can also be used where N_T is the total number of target atoms per volume in the material being activated, σ_{act} is the microscopic activation cross-section. When equations 1 and 2 are combined, the rate of activation can be expressed as

$$R = \phi \sigma_{act} N_T . \qquad [3]$$

Activated material is removed via decay by emission of gamma rays and beta particles. A sample activates and decays concurrently and these two competing processes determine the activity at any point in time. The rate of decay is given by λN, where λ is the decay constant, and N is the number of radioactive nuclei. The rate of change in N is the difference between the rate of activation, R, and the rate of decay (10) or

$$dN/dt = R - \lambda N. \qquad [4]$$

When a thin foil of the target atoms is placed in a neutron flux, its activity increases exponentially until the activity reaches a saturation value. The foil's activity becomes saturated when the rate of creation of a radionuclide equals the rate of its radioactive decay. Therefore this induced activity builds up with time and approaches a saturated activity given by (9)

$$R = \lambda N . \qquad [5]$$

Assuming $N = 0$ at time $t = 0$, equation 4 can be integrated to yield (8)

$$N(t) = \frac{R}{\lambda}(1 - e^{-\lambda t}) . \qquad [6]$$

If activation is not carried out to saturation, the activity, A, of the foil is given by

$$A(t) = \lambda N(t) = R(1 - e^{-\lambda t_0}) . \qquad [7]$$

To measure the activity resulting from exposure to the neutron flux, the foil is transferred to a detector. Once removed from the neutron flux the activity of the foil is continually decaying and account must be made for the time during each step. As shown in Figure 1, if the counting is carried out over an interval between t_1 and t_2, the number of counts measured will be (8)

$$C = \varepsilon \int_{t_1}^{t_2} A e^{-\lambda t} dt + B$$

$$C = \varepsilon \frac{A}{\lambda}(e^{-\lambda t_1} - e^{-\lambda t_2}) + B \qquad [8]$$

where ε is the overall counting efficiency and B is the number of background counts expected in (t_2-t_1).

By combining equations 7 and 8 we obtain equation 9 for the saturation activity (8)

$$A = \frac{\lambda(C - B)}{\varepsilon(1 - e^{-\lambda t_0})(e^{-\lambda t_1} - e^{-\lambda t_2})} . \qquad [9]$$

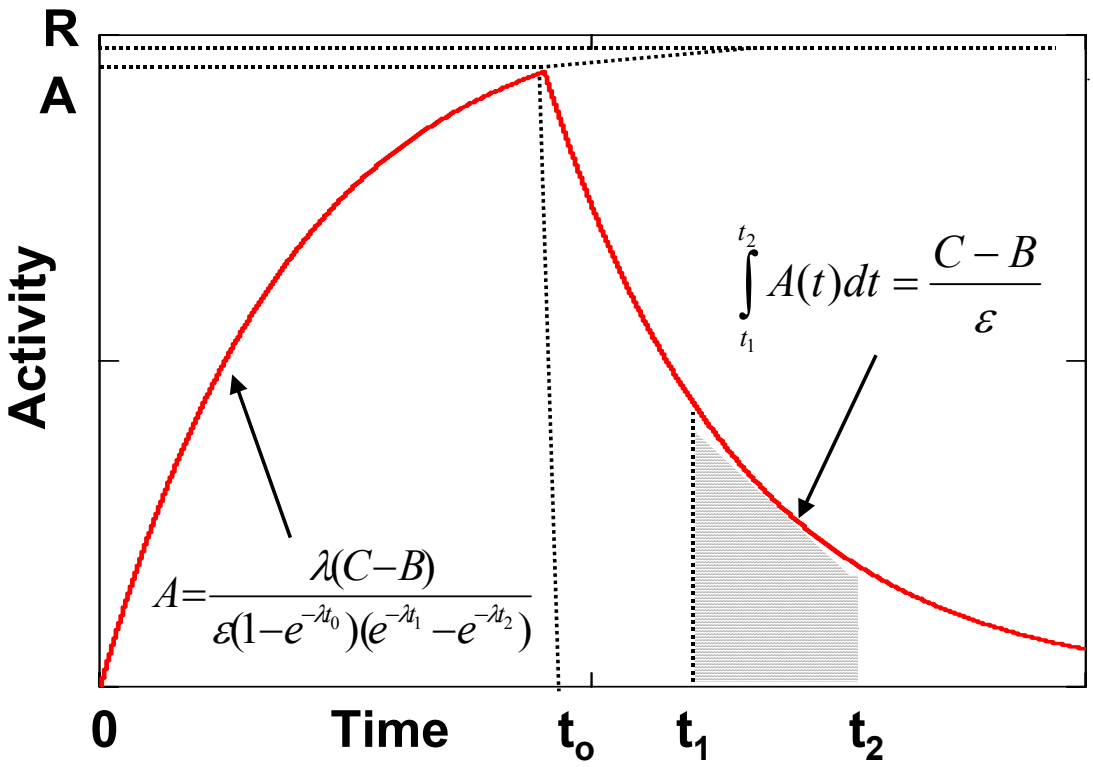

Figure 1 Activity of an activation foil where t_o is the time of the foil's removal from the neutron flux. The foil's activity is counted between t_1 and t_2. (8)

Correction Factors

Many factors go into defining the overall counting efficiency. If each factor is accounted for, the measured counts can be adjusted to accurately reflect the true activity.

The counter geometry correction factor, f_g, corrects for the fraction of the radiation that is not subtended by the detector and is defined as

$$f_g = \frac{\Omega}{4\pi}, \qquad [10]$$

where Ω is the solid angle that is subtended by the detector.

To determine the solid angle, a point source that emits radiation isotropically is used. A cone, as shown in Figure 2, is projected from the source and intersects an imaginary sphere that surrounds it, which defines the solid angle. The solid angle can be expressed as,

$$\Omega = \int_0^{2\tan^{-1}\left(\frac{a}{d}\right)} \int_0^{2\tan^{-1}\left(\frac{a}{d}\right)} \sin(\theta)\, d\theta d\phi \,, \qquad [11]$$

where a is the radius of the detector and d is the distance between the source and the detector.

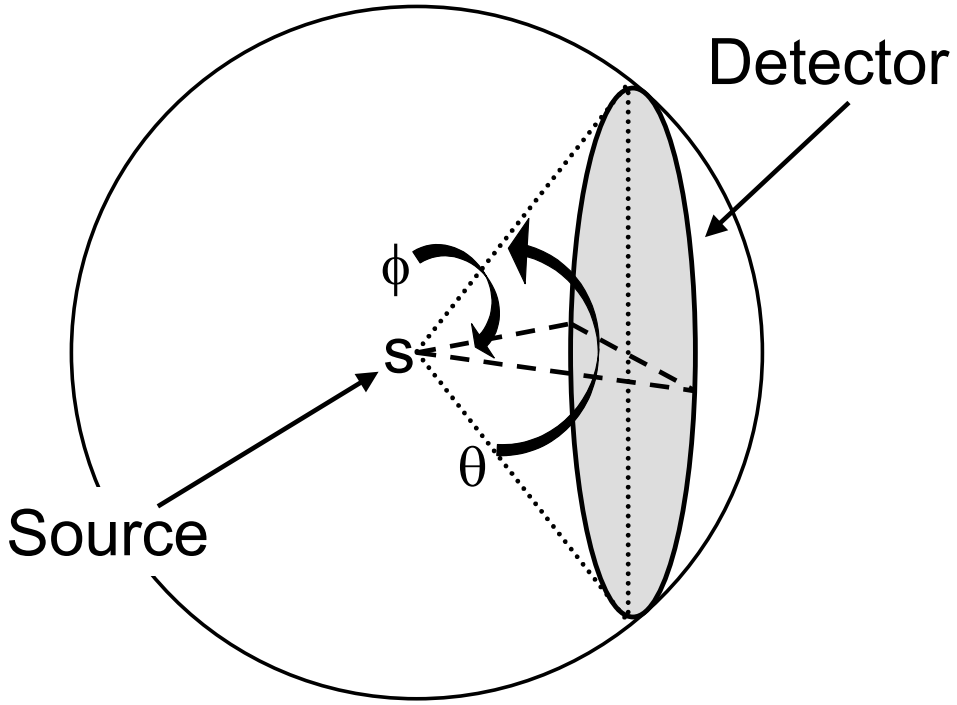

Figure 2 The definition of a solid angle.

Figure 3 shows the source and detector geometry used in this thesis for the detection of both gamma and beta radiation. The assumptions behind this geometry include a

uniform circular disk, emitting radiation, aligned on the same axis as the detector. To determine the solid angle for the distributed source, an additional term was added to equation 11. The additional term defines the average solid angle subtended by the detector across the surface of the distributed source. The solid angle for a distributed source is defined as

$$\Omega = \int_0^S \int_0^{2\tan^{-1}\left(\frac{a}{d}\right)} \int_0^{2\tan^{-1}\left(\frac{a}{d}\right)} \sin(\theta) \frac{\cos\left(\tan^{-1}\left(\frac{s`}{d}\right)\right)}{s} d\theta d\phi ds`,$$

where $s`$ is the radius of the distributed source that is being integrated and s is the radius of the distributed source.

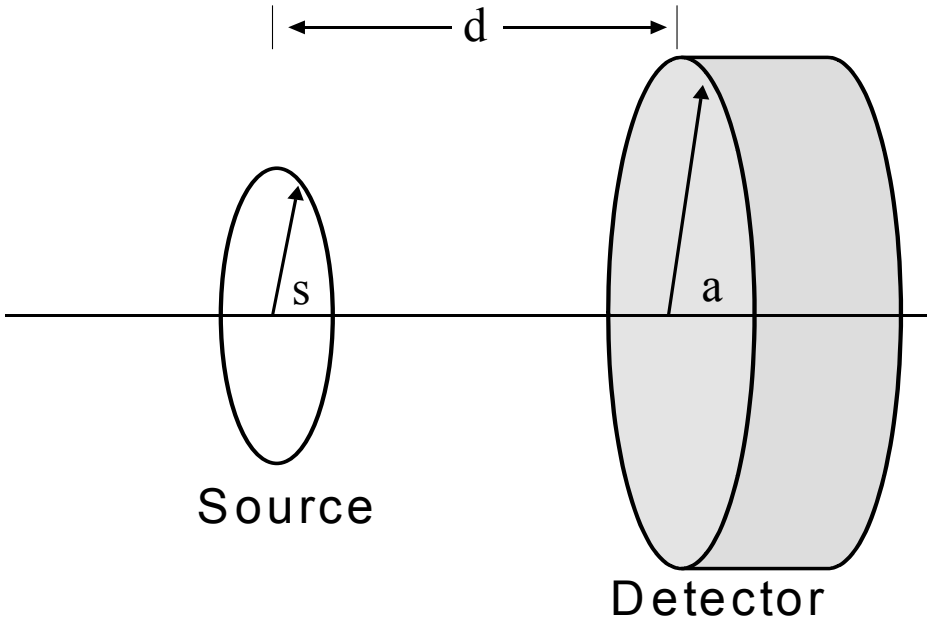

Figure 3 The source-detector geometry used to find f_g (8)

The counter-window correction factor, f_w, corrects for the number of beta particles or gamma rays absorbed or scattered by the detector window. The detector efficiency includes this correction factor. (11)

Backscattering of beta particles from surrounding materials can increase the count rate. If the foil is much thinner than the range of the beta particle, the source mount or other surrounding materials can contribute to the beta backscatter. During counting, the foil sat directly upon the detector cover and supporting material, Plexiglas, was placed on top of the foil to keep the foil flat. The correction factor for beta particle backscattering from the foil support material, f_{bs}, was found by the ratio of the counts from a bare foil and the counts from a foil covered with the Plexiglas supporting material. (10) The value for f_{bs} was found to be unity.

The intrinsic efficiency is determined experimentally. The counter efficiency for beta particles, f_e is considered unity.

The foil itself can reduce the number of counts measured by absorption or scattering. The beta particle self-absorption correction factor, f_a, is strongly dependent on the foil thickness. The absorption increases rapidly with increasing thickness for thin foils because of the absorption of low energy beta particles. The absorption of thermal neutrons decreases the neutron flux as it passes through increasing thickness of foil. Equation 12 is an empirical formula that provides this correction factor, (11)

$$f_a = \frac{1}{t\mu}(1 - e^{-\mu t}), \qquad [12]$$

where t is the thickness of the activation material and μ is the attenuation coefficient. The absorption of gamma rays by the foil also increases with thickness. Equation 13 is an empirical formula that yields the gamma self-scattering correction factor (f_γ), (12)

$$f_\gamma = 1.0 + \frac{t}{239.5}, \qquad [13]$$

where t is the thickness of the foils in mils.

All of the correction factors are combined to adjust the activity. The corrected activity for the gamma detector is given by

$$A_{sa} = A_{CS} f_\gamma f_w f_g f_{bs} \varepsilon_{\text{int}} \qquad [14]$$

and the corrected activity for the beta detector is given by

$$A_{sa} = A_{CS} f_a f_w f_g f_e f_{bs} \varepsilon_{\text{int}}, \qquad [15]$$

where A_{cs} is the corrected saturated activity from equation 9, and ε_{int} is the intrinsic efficiency of the appropriate detector.

Cadmium Difference Theory

The saturation activity can be divided into the activity contributed by thermal neutrons and that contributed by epithermal neutrons, (11)

$$A_\infty = A_{\infty(th)} + A_{\infty(e)} \qquad [16]$$

A cadmium cover absorbs most thermal neutrons while allowing epithermal and fast neutrons to irradiate the foil. The cover thickness is chosen so it is slightly larger than the mean free path of a thermal neutron in cadmium. By irradiating the foils with and without the covers one can measure the difference in activity induced by only epithermal

neutrons and activity induced by all neutrons. The difference represents the thermal activity. As shown in Figure 4, cadmium absorbs some epithermal neutrons. This necessitates the application of the correction factor, F_{Cd}, to correct for the epithermally-induced activity. (11) The correction factor is dependent upon the cadmium cover thickness. For the 20 mil cadmium covers used in this thesis F_{Cd}=1.056. (10) Including the correction factor, equation 16 can be rewritten as

$$A_{th} = A_{\infty} - F_{Cd} A_{\infty Cd} . \qquad [17]$$

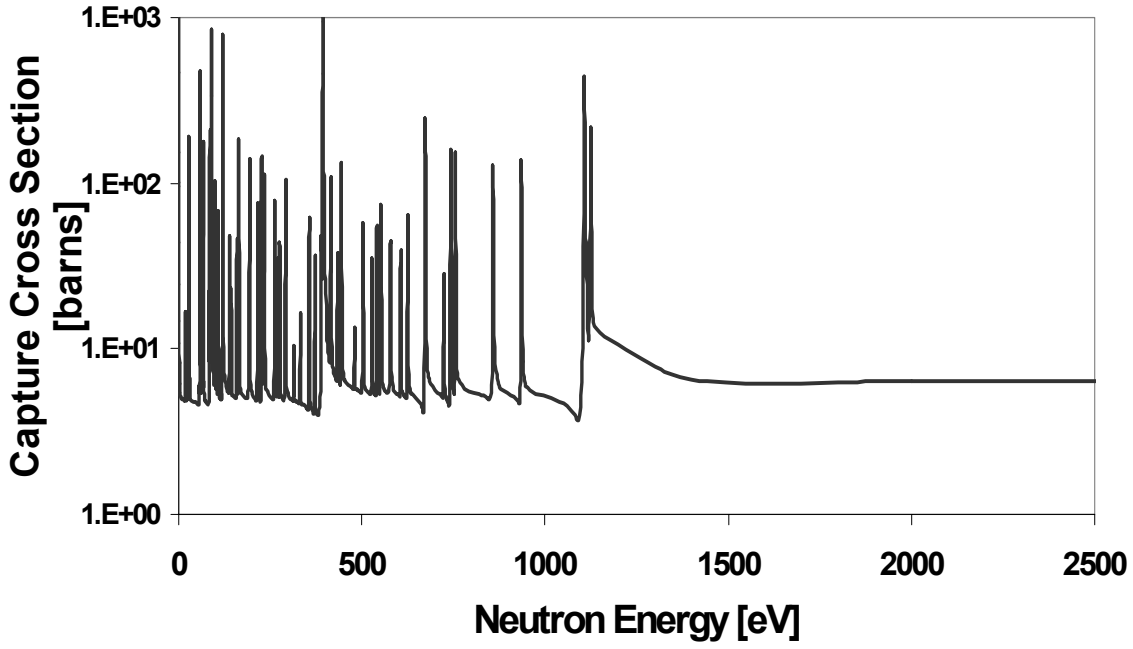

Figure 4 The capture cross section of cadmium which shows the absorption of epithermal neutrons. (13)

Time Dependence

When a thin foil is placed in a neutron flux, the induced activity increases exponentially as shown in equation 7. Assuming the neutron flux is constant, the induced activity changes with time during the time dependent phase. Once enough time has

passed, usually about ten half-lives, the induced activity reaches a steady state called saturation. At saturation the activity changes only if the flux changes.

If saturated, the measured activity from a single activation foil can be used to calculate the flux using equation 3. The measured activities from a time-dependent foil, using the calculated flux from the saturated foil, can be compared to a theoretical model, based upon knowledge of the material parameters, to determine if the neutron source has been removed during the foil exposure. If the activities vary outside of a user-specified error tolerance, the neutron source has been removed. An ideal combination of foils will maintain at least one saturated and one time-dependent foil over an extended monitoring period. Different combinations of foils would be needed as different isotopes enter saturation. More time-dependent curves give redundancy and increase the accuracy of the detector system.

Figure 5 shows an example foil combination where foils are in different stages of activation. The rectangle highlights the activities of each foil at a specific time period. The rectangle's width varies with the measured activity error. If the measured activity is within tolerance, some certainty exists that the neutron source has not been removed during the monitoring period. If only some or none of the measured activities are within tolerance then there is uncertainty that the neutron source has remained undisturbed throughout the monitoring period.

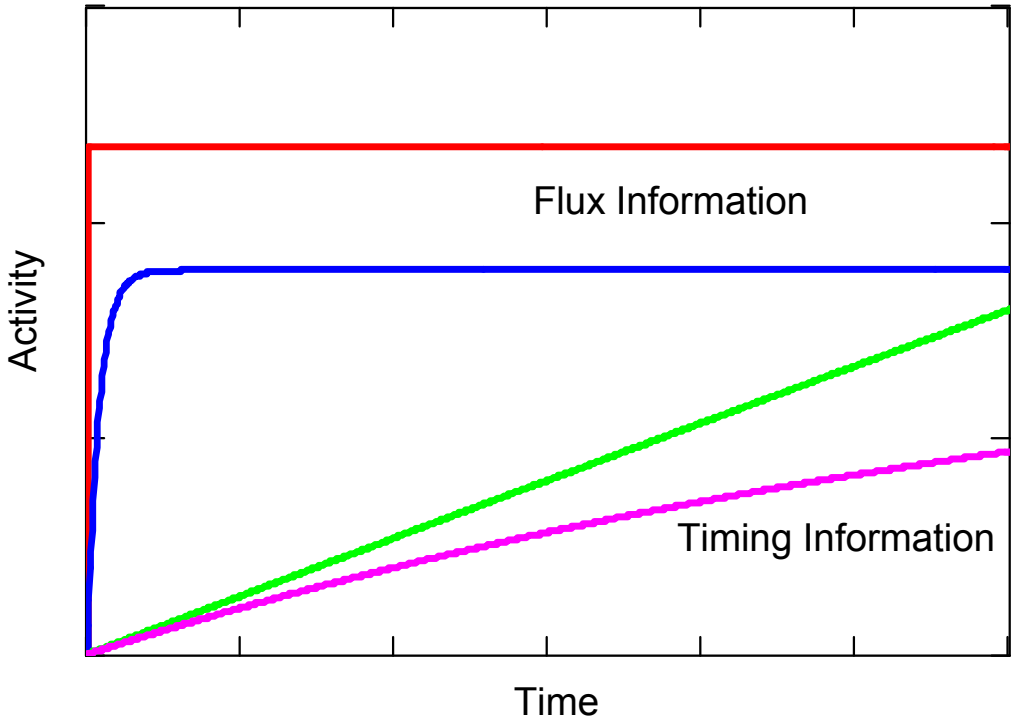

Figure 5 Example foil detector system with foils in different stages of activation. The activities in the rectangle are used to determine if the neutron source has been removed.

Detectors

The detectors below were chosen for their availability and ability to detect low gamma and beta activity.

Canberra Model GC10021 High Purity Germanium

The Canberra Model GC10021 High Purity Germanium (HPGe) detector is a p-type, closed-end, coaxial detector that detects gamma activity from low activity foils in a high and low background. The crystal has a diameter of 83 millimeters and a length of 84.5 millimeters and is located 5 millimeters from the detection window. An HPGe detector collects electrical charges created at either boundary of the semiconductor material and records these pulses and differentiates between energies.

HPGe detectors have superior energy resolution and high efficiency. Figure 6 shows the experimentally determined gamma intrinsic efficiency for the detector used in this study, which is based upon an energy spectra measurement from a known multinuclide source. The error associated with Figure 6 ranges from 2.2 to 6.0 percent depending upon energy. The gamma energies emitted by the radioactive isotopes used in this thesis fall into the HPGe's greatest efficiency range of 100 to 1000 keV. Annex E depicts the gamma intrinsic efficiency at each energy.

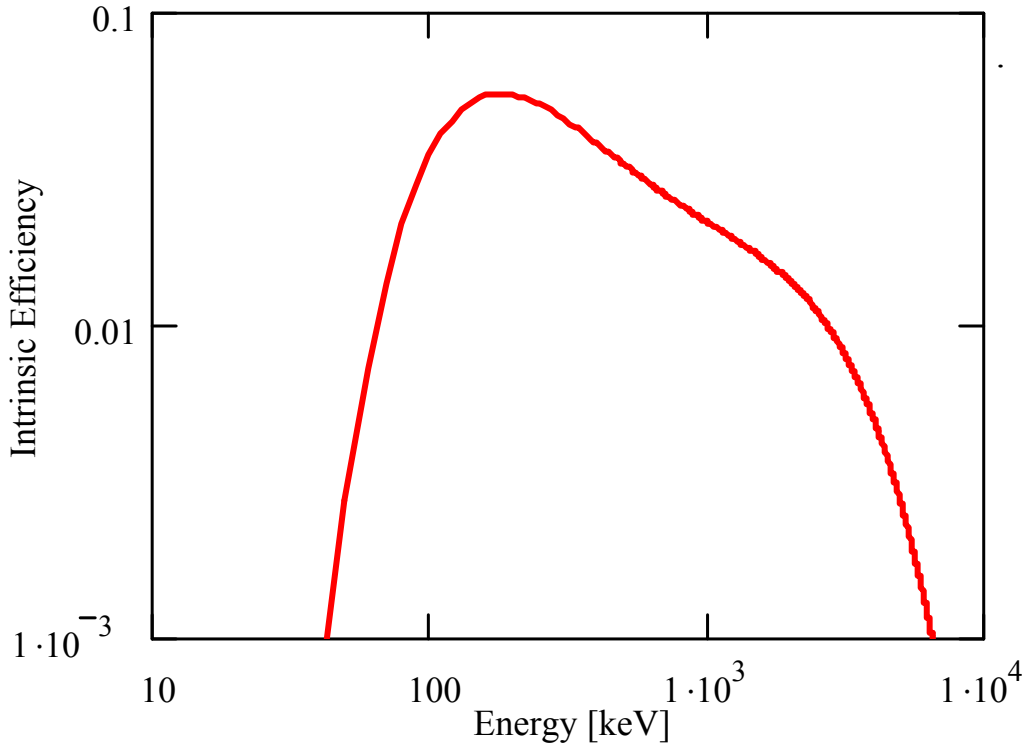

Figure 6 Gamma Intrinsic Efficiency vs. Gamma Energy (14)

Canberra Model 2400 Alpha/Beta System

The Canberra Model 2400 Alpha/Beta system has the ability to measure very low counts from beta radiation. The system has a dual gas proportional pancake detector

assembly, which captures radioactive emissions from the sample. The detector system gives almost a 2π configuration that consists of a large area (12.7 centimeters x 16.2 centimeters) guard detector and a 5.7-centimeter diameter, window area, thin-window sample detector. The sample detector captures the electronic pulses while the guard detector detects background radiation, which typically comes from cosmic radiation, lead x-rays, or gamma radiation from the sample. The guard detector operates in an anticoincidence mode with the sample detector to eliminate counting unwanted radiation resulting in an extremely low background counting system. (20)

Ludlum Measurements Model 12-4 Neutron Counter (Bonner Sphere)

The Ludlum Model 12-4 Neutron Counter was chosen for its ability to measure neutrons and was used to verify the calculations and procedures that were performed using activation foils.

BF^3 gas proportional detectors are efficient only for thermal neutrons. The capture cross section of high-energy neutrons is very small so the neutrons must be slowed for detection. The calculated efficiency for a BF_3 tube is about 90 percent at thermal energies but drops to about 4 percent at 100 eV. (8) By surrounding a gas proportional detector with a hydrogen-rich moderator, higher energy neutrons are slowed to thermal energies and can be detected efficiently. The Ludlum Model 12-4 is a 1.6-centimeter diameter by 2.5-centimeter thick BF^3 detector surrounded by a 9-inch diameter cadmium loaded polyethylene sphere. The Ludlum Model 12-4 measures neutrons with energies ranging from thermal through 10 MeV. (15)

Expected Flux - Fetter Model

The magnitude of the neutron flux from a hypothetical, unclassified, general characteristic nuclear weapon within a storage container was required. Fetter et. al. developed four models that defined a range of radiation outputs emitted by nuclear

warheads. This thesis used the nuclear weapon model that has a 4 kg WgPu hollow sphere and the highest escaping neutron flux for the theoretical neutron source. (6) A beryllium neutron reflector surrounds the fissile material to reduce its neutron losses, thereby reducing the amount of fissile material required for critical mass. The model design requires the placement of a 52 kg depleted uranium tamper between the chemical explosives and the fissile material. The tamper shapes inward momentum from the chemical explosives and also serves as an additional neutron reflector. An aluminum case holds the model together.

Figure 7 portrays the Fetter Model with the Rocky Flats shipping container. The Fetter model describes only the nuclear weapon's physics package. To describe a flux on the outside of a storage container, the model must include the missile and the storage container. Graphite, a neutron moderator, represents the missile. The shipping containers used at Rocky Flats provide the dimensions of the theoretical storage container. (16) No documentation could be found identifying the composition of the interior of the shipping container so paraffin, another neutron moderator, substitutes for the model's interior. Stainless steel reinforces the outside of the shipping container.

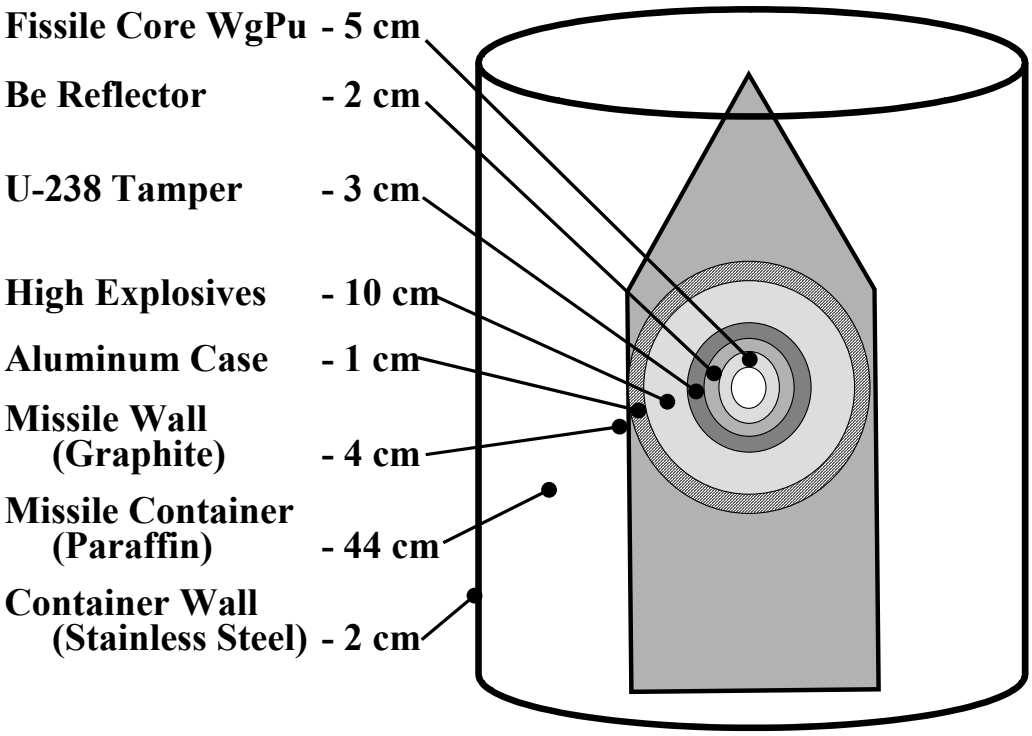

Figure 7 The dimensions and component composition of the Fetter model inside the Rocky Flats shipping container (6)

Fetter et. al. reported the neutron emission rate at the surface of the physics package was 400,000 n/sec with a flux of 70 n/cm^2-sec.(6) Using only the macroscopic absorption cross section (attenuation due to scattering was omitted) and the flux at the surface of the Fetter model, the neutron flux at the surface of the storage container was determined after it had been attenuated by 4 centimeters of graphite, representing the surface of the missile, 44 centimeters of paraffin, representing the interior of the container, and 2 centimeters of iron, representing the exterior surface of the container. The neutron flux at the surface of the storage container was estimated at 0.5 n/cm^2-sec, which this thesis refers to as the target flux. Figure 8 shows the location of the calculated neutron fluxes.

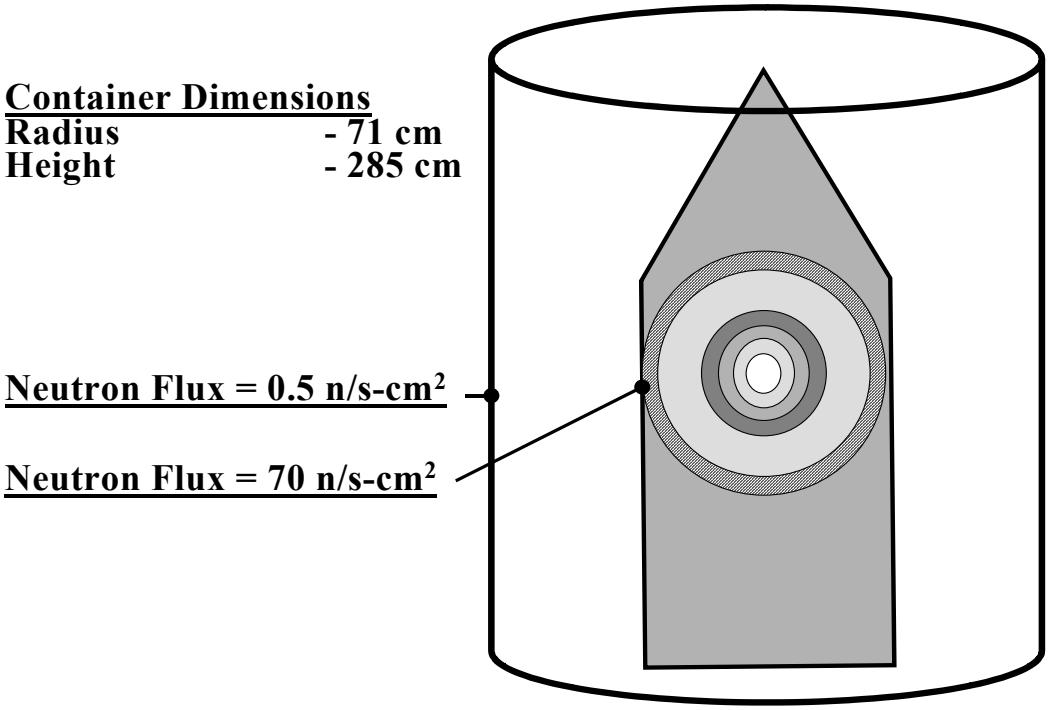

Figure 8 The neutron flux on the outside of the Rocky Flats shipping container containing the Fetter model's physics package (6)

Neutron Source

WgPu is defined as plutonium that contains less than 7 percent of the spontaneously fissioning isotope ^{240}Pu. Taking into account the presence of ^{238}Pu, ^{241}Pu, and ^{242}Pu, the percentage of ^{239}Pu is about 93 percent. The even-numbered isotopes of plutonium, ^{238}Pu, ^{240}Pu, and ^{242}Pu, spontaneously fission at a rate of 1100, 471, and 800 SF/gram-second respectively. Odd-numbered plutonium isotopes spontaneously fission at a much lower rate ranging from 0.0003 to 0.006 SF/gram-second. (6)

For the neutron source used in laboratory experiments, this thesis used a plutonium-beryllium (PuBe) source. A PuBe source generates the majority of its neutrons from (α,n) reactions. Figure 9 shows the PuBe energy spectrum including ^{239}Pu^{9}Be(α,n); the multibody break-up reaction ^{9}Be(α, αn)^{8}Be; the secondary interactions ^{9}Be(n,2n); and ^{239}Pu(n,f). (17) Figure 9 portrays a comparison of energy spectra from three different 10

Curie PuBe sources. These sources agree well above 2 MeV. At energies below 2 MeV one source differs from the other two. No information exists to determine which spectrum most resembles the PuBe source on hand.

This thesis focused on thermal neutrons and assumed that most neutrons in the laboratory experiments were thermalized when they reached the activation foils because they passed through 13.5 centimeters of paraffin, a neutron moderator. To further limit the influence of high-energy neutrons, all activities were adjusted to reflect only the activity that was a result of thermal neutrons.

The author did not have access to a WgPu neutron spectrum. However because this thesis limited its scope to thermal neutrons and the WgPu neutrons must pass through an estimated 71 cm of material of varying compositions and densities to escape from a storage container, the difference in the energy spectrums between WgPu and PuBe is neglected.

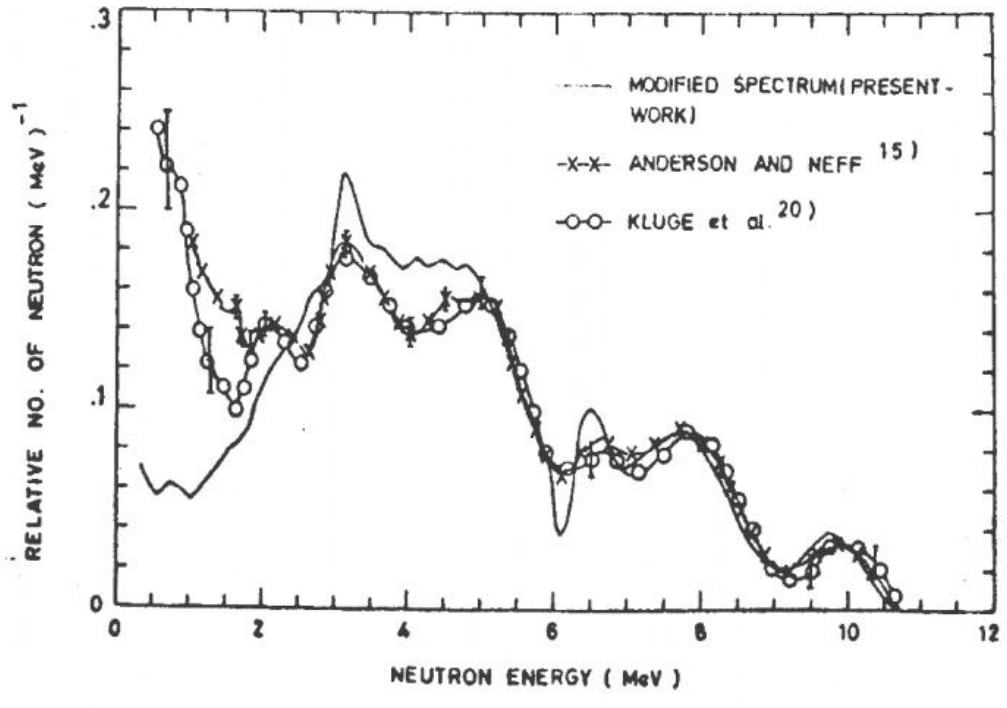

Figure 9 Comparison of neutron spectrum from 10 Ci PuBe sources (17)

III. EXPERIMENT

This chapter contains three sections. The foil section gives information and statistics for the foils considered in this thesis. The theoretical section shows the methodology and activation theory used to investigate the effects of background on activation foils. The laboratory experiments section provides the methodology and experimental set-up for the testing of the limits of detection.

Foil Information

This thesis limited its focus to five activation foil materials; silver, gold, indium, europium, and gadolinium. The foils examined emit gamma rays and beta particles following activation. Annex D shows the decay diagrams for all of the foils studied.

An ideal foil for low flux measurements has a large absorption cross section and emits a single beta particle and gamma ray or cascade of gamma rays for each decay with no alternate decay pathways. If two different types of radiation are emitted from the same reaction, two independent detection means can be used to determine the activity. A single decay scheme allows for efficient collection of the decay signal.

Silver

Silver was chosen because of its availability for laboratory testing, the large thermal neutron cross section of 91 barns for ^{109}Ag and the long 250 day half-life of its daughter $^{110}Ag_m$.

Natural silver consists of 52 percent ^{107}Ag and 48 percent ^{109}Ag. ^{107}Ag has a thermal neutron capture cross section of 39 barns. (18) Of the four possible neutron absorption reactions, there are two reactions of interest. One reaction, $^{107}Ag \rightarrow ^{108}Ag_m$ has a half-life of 130 years and produces three gammas, 434 keV, 614 keV, and 722 keV, when it decays. $^{108}Ag_m$ does not beta decay. A second reaction, $^{109}Ag \rightarrow ^{110}Ag_m$ has a half-life of

250 days and produces two key gammas, 658 keV and 885 keV and a 3 MeV beta particle when it decays. (19)

Gold

Gold was chosen because of the extensive amount of previous work available on the activation of gold, its availability for laboratory testing, its natural composition as a single stable isotope, its single decay chain with a nearly simultaneous emission of a single monoenergetic gamma and beta particle, and the large thermal neutron cross section of 98.7 barns for ^{197}Au.

The activation product, ^{198}Au, decays with a half-life of 2.7 days. (18) In 99.98 percent of its decays, ^{198}Au decays with beta emission to an excited state of mercury. In approximately 95 percent of the decays, the excited mercury atom emits a 411 keV gamma ray. (19)

Indium

Indium was chosen because of the large amount of previous work available on the activation of indium, its availability for laboratory testing, the 54 minute half life of $^{116}In_m$ which lends itself to multiple laboratory experiments in a condensed period of time, and ^{115}In's large thermal neutron cross section of 162 barns.

Natural indium consists of 4 percent ^{113}In and 96 percent ^{115}In. ^{113}In's contribution to total activity is negligible due to its low isotopic abundance and small cross section. (18) Of the four possible reactions with neutron absorption, there is one reaction of interest. The reaction $^{115}In \rightarrow ^{116}In_m$, produces three key gammas, 417 keV, 1097 keV, and 1294 keV, and a 1 MeV beta particle when it decays. (19)

Europium

Europium was chosen because of ^{151}Eu's relatively large thermal neutron cross section. Extreme hazards exist when working with europium metal. Europium ignites in air at about 150°C to 180°C. It is the most reactive of the rare-earth metals, quickly oxidizing in air. For this reason laboratory experiments were not performed using europium metal.

Natural europium consists of 48 percent ^{151}Eu and 52 percent ^{153}Eu. (18) Of the four possible reactions with neutron absorption, there are three reactions of interest. The reaction $^{151}\text{Eu} \rightarrow ^{152}\text{Eu}$ has a cross section of 5900 barns and a half-life of 13.5 years, produces three key gammas, 122 keV, 344 keV, and 1408 keV, and a 0.7 MeV beta particle when it decays. The reaction $^{151}\text{Eu} \rightarrow ^{152}\text{Eu}_m$ has a cross section of 3300 barns and a half-life of 9.3 hours, produces two key gammas, 842 keV and 963 keV, and a 1.9 MeV beta particle when it decays. The reaction $^{153}\text{Eu} \rightarrow ^{154}\text{Eu}$ has a cross section of 320 barns and a half-life of 8.5 years, produces two key gammas, 122 keV and 1275 keV, and two beta particles, 0.58 MeV and 0.27 MeV, are produced when it decays. (19)

Gadolinium

Gadolinium was selected because of the huge thermal neutron cross section of ^{155}Gd and ^{157}Gd's. However, both isotopes are only present in low concentrations of natural gadolinium and following neutron absorption both lead to stable isotopes. (18) Gadolinium metal oxidizes in air and was not used for laboratory experiments.

Owing to the large cross section for gadolinium, it can be used in a similar manner as cadmium in differentiating neutron energies. Gadolinium will preferentially absorb neutrons at energies below 10 keV. (19)

Theoretical Analyses

This section investigated the affects of various background environments using activation theory. Though this section is theoretical, the detector responses were based upon the responses recorded from the Canberra Model GC10021 High Purity Germanium (HPGe) detector for gamma detection and the Canberra Model 2400 Alpha/Beta (beta) detector system for beta detection. The author assumed that a constant flux activated the foils for two years and once retrieved the foils were counted for one hour.

Gamma Backgrounds

To achieve a consistent high background environment, the HPGe detector was operated inside a tomb composed of lead bricks and lined with cadmium. The tomb absorbs most cosmic radiation before it reaches the detector but a neutron source had activated the interior of the tomb causing a constant elevated background.

A low background environment was achieved by placing the same detector in a new model 747 Canberra Lead Shield. The shield prevents high background counts and interference by lead x-rays by using a four-inch thick lead wall and a 1.0-millimeter tin and 1.6-millimeters copper graded liner. (20)

Standard for Detection

Calculations were performed comparing the effects of a high versus low background for the HPGe detector. A 12-hour background was run with the same HPGe detector in a high background tomb and in the low background tomb. A gamma spectrum was gathered and focused on the key energy of the emitted gamma ray. This thesis defines key gamma energies as gamma rays with energies that have a relative intensity greater than 25 percent of the largest intensity peak emitted. Owing to the Gaussian spread and detector resolution, a region of interest (ROI) was placed at ±0.5 keV. Ten one-hour background counts determined the standard deviation of each key energy ROI.

The beta detector system suppresses background via an anticoincidence system and shielding. Therefore, only a 12-hour low background run was needed for the beta detector. Ten one-hour background counts were run with the beta detector to determine the standard deviation.

Estimates of the limits of detection for each of the detector environments are based on the standard deviations determined experimentally for the backgrounds. Counts greater than three standard deviations above the average background were considered detectable. For a Gaussian distribution of the background, 99.7 percent of the background measurements will fall within three standard deviations of the average value. Therefore, the probability is just 0.003 that a count that exceeds the average background count plus three standard deviations is caused by the background rather than another source.

From the background data the background rate was found. Table 1 holds the ranges for the minimum number of counts to be considered detectable for both the HPGe and beta detectors. The experimentally determined intrinsic efficiency for the beta counter was 24 percent at 1500 volts.

Table 1 Minimum number of detectable counts for HPGe and Beta detectors per hour

	Low Background	**High Background**
HPGe at 103 keV	24 counts/hour	230 counts/hour
HPGe at 1408 keV	4.0 counts/hour	24 counts/hour
Beta Detector	8 counts/hour	N/A

Minimum Flux

A standard one-mil thick foil was assumed for all calculations. Additionally, each standard foil had a radius of five-centimeters. Equation 8 defines the absolute number of counts expected, following activation.(8) For each background, detector, and energy the

minimum number of counts required to be detected was determined for the standard, isotopically-pure foil. The flux in equation 8 was solved for which produced,

$$\phi = \frac{C\lambda}{\varepsilon \Sigma V (e^{-\lambda t_1} - e^{-\lambda t_2})}, \qquad [18]$$

which gives the minimum flux required to achieve counts greater than three standard deviations plus background.

Minimum Time to Detect a Flux

The fluxes of 1, 70, 200, and 1000 n/cm^2-sec were used to determine when an activity could be detected in excess of background. To draw timing information from activated foils in a specific flux, the author determined the minimum foil activation time before the activity was high enough to be detected. The minimum detectable count in excess of background determines the minimum activity in one hour required for detection. The activation time for attaining the minimum activity, A_{min}, was found by use of equation 7 and does not include decaying while counting.

$$A_{\min} = \phi \sigma N_T (1 - e^{-\lambda t_{\min}}) \qquad [19]$$

Solving equation 19 for the minimum time, t_{min}, results in,

$$t_{\min} = \frac{-\ell n \left[\frac{\phi \sigma N_T - A_{\min}}{\phi \sigma N_T} \right]}{\lambda}, \qquad [20]$$

which is the minimum time required to detect a specific flux with a specific foil containing N_T atoms.

The Timing of a Detector System

Once minimum activation times were established for each of the foils studied, the activation curves were combined as shown in Figure 5. The goal of combining the multiple foils was to have a minimum of one saturated and one time-dependent foil detectable through out the lifetime of the analysis. The flux was determined using the measured activity of the saturated foil and solving for ϕ using equation 3. The timing information was determined using the newly computed flux and graphing activity versus time using equation 7 for each isotope.

The detection of the activity associated with each isotope depends upon the flux and the counting background. The author focused on the fluxes of 70, 200, and 1000 n/cm^2-sec but a wide variety of fluxes including 1, 7, 15, 32, 500, 2000, 1x10^4, 1x10^5, and 1.8x10^6 n/cm^2-sec were investigated.

When a new isotope became detectable it was included in the graph. These graphs were used to develop the timing coverage information. These graphs identified the gaps in detection coverage when the foils were used as a detection system at varying fluxes.

Laboratory Experiments

In this section several experiments were performed to investigate the neutron detection capability using gold, silver, and indium activation foils. The same detectors were used as in the theoretical section.

Neutron Source and Procedure Validation

The PuBe source used in this experiment, M-1170 known locally as T00303, had an original neutron emission rate of 9.04x10^6 n/sec on March 9, 1962. (21) The

corresponding flux at the surface of the source was $1.06 \times 10^5 \pm 1.2 \times 10^3$ n/cm^2-sec. ORIGEN, a Monte Carlo based program, included neutrons from both fission and (α,n) reactions to age the PuBe source to November 27, 2002 and was used to determine the flux as $8.0 \times 10^4 \pm 940$ n/cm^2-sec. ORIGEN's calculation error was unknown resulting in an underestimation of error. The calibrated Bonner Sphere measured the neutron flux at the mouth of the PuBe storage container. After translation of the dose to flux and corrections due to solid angle, the thermal neutron flux was determined as $7.9 \times 10^4 \pm 2.4 \times 10^4$ n/cm^2-sec with the majority of the error resulting from error in reading the dose off the Bonner Sphere gauge.

An experiment was performed to verify the procedures and calculations used to determine the thermal neutron flux from the activity of a gold foil. Two bare and two cadmium-covered gold foils were placed at the mouth of the conical PuBe storage container that was approximately 18 inches high with a hollow center core that was approximately 14 inches deep and 4 inches in diameter, where the PuBe source was stored. The hollow center was surrounded by approximately 5 inches of paraffin. Figure 10 shows the experimental set up. The thermal neutron flux was determined as $7.5 \times 10^4 \pm 4.7 \times 10^3$ n/cm^2-sec, which is within the known error of the values determined by ORIGEN. The ORIGEN values and those obtained with the Bonner Sphere validate the procedures used for determining the thermal neutron flux from activation foils. The author assumed that the calculations and procedures used for gold were applicable to indium and silver with minor adjustments for efficiency and composition.

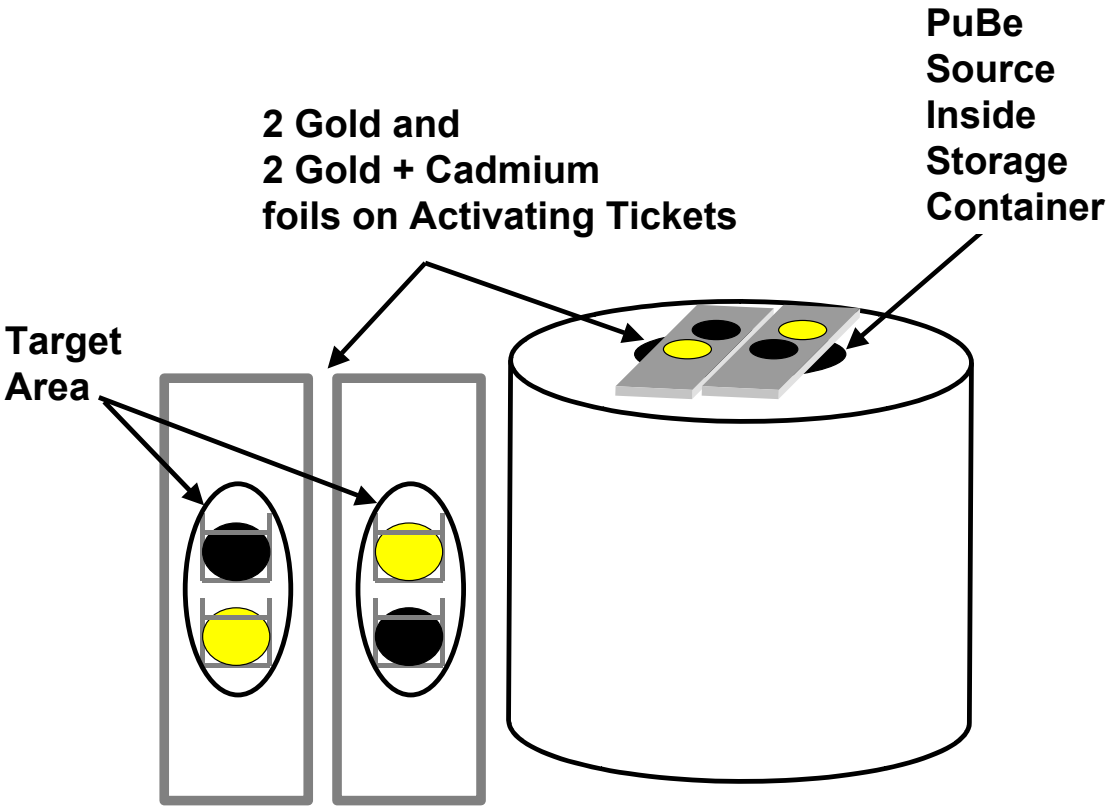

Figure 10 Experiment set-up for procedure verification experiment

Experimental Set-up and Procedure

The concept was to mimic some characteristics of the Fetter physics package inside the Rocky Flats shipping container while attempting to achieve a thermal neutron flux of about 70 n/cm^2-sec at the target area. The experimental set-up used is shown in Figure 11. To reduce unnecessary exposure, the PuBe source remained inside its storage container. The paraffin plug was removed and the PuBe storage container was placed on its side with the opening at the same height as the center of the activating tickets. The neutrons from the PuBe source, representing the Fetter model, passed through 0.5 inches of stainless steel, representing the outside of the missile, 13.5 centimeters of paraffin, representing the interior of the storage container, and one inch of stainless steel representing the shell of the storage container. Because of structural limitations, a three-

inch air gap existed between the PuBe source container and the first stainless steel block and a two-inch air gap existed between the last stainless steel block and the activating tickets that held the test foils.

Figure 12 shows how the activating tickets from Figure 10 and 10 held the foils during activation. The activating tickets had a shallow pocket of Plexiglas, which held the bare foils. The cadmium-covered foils were taped directly above the bare foils. The wire loop on the top of each ticket allowed for quick and easy removal from the flux to reduce exposure.

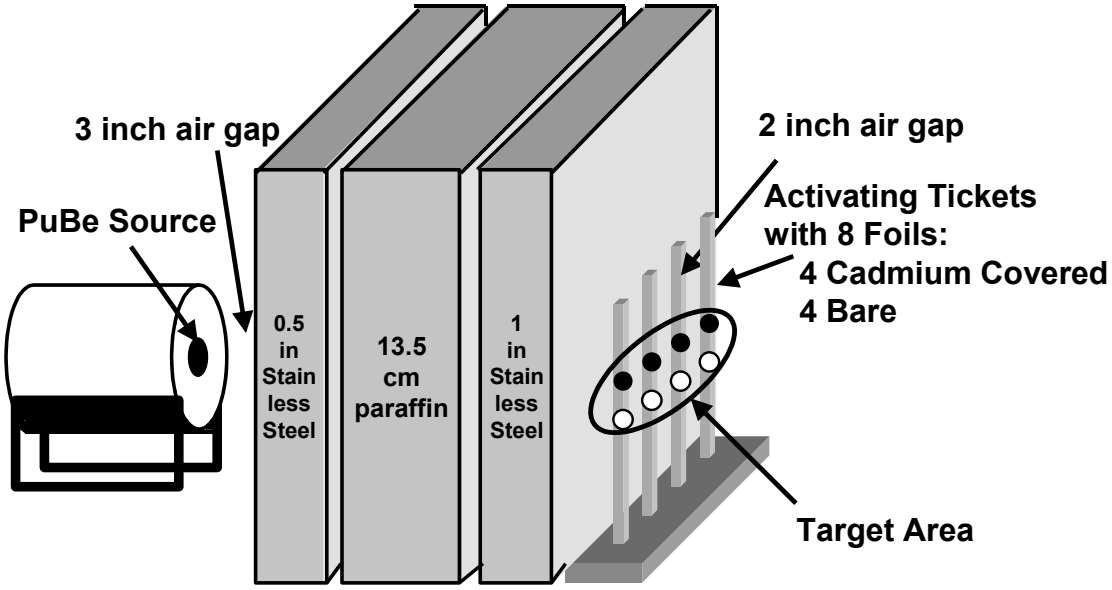

Figure 11 Experimental Set-Up Mimicking Characteristics of the Fetter Model Inside the Rocky Flats Shipping Container

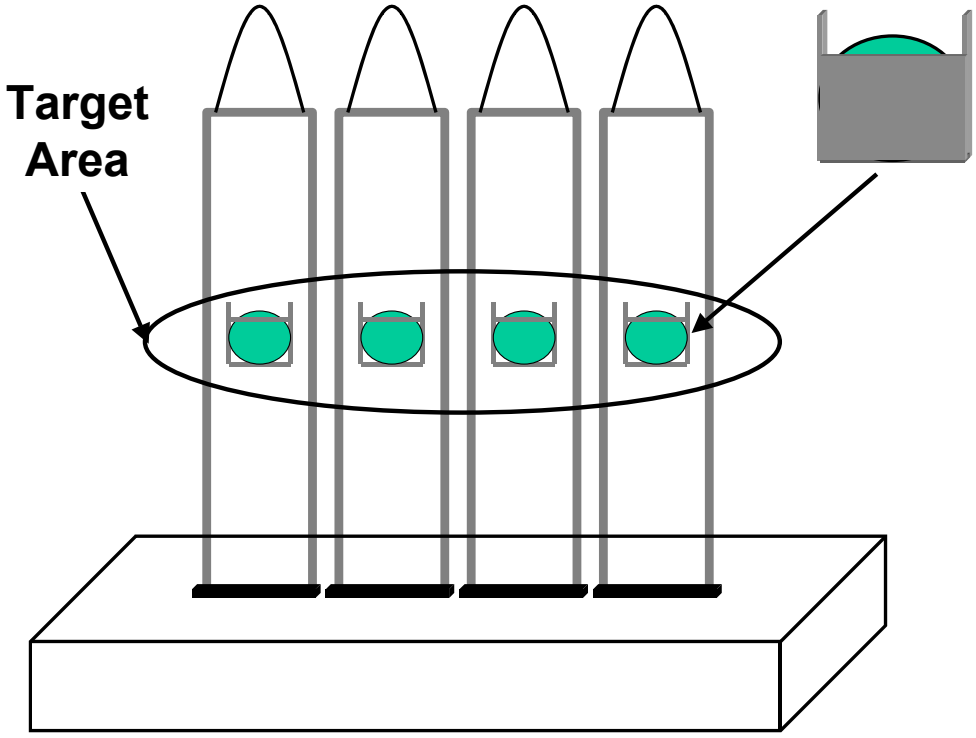

Figure 12 Activating tickets with four foils in target area

The experiments included two foil sizes. The small foils are circular with a radius of 0.5 centimeters. The large foils are a one-inch by two-inch rectangle. Each foil was weighed and placed on an activating ticket. The tickets were placed with the foils facing the neutron source and exposed for a specified time. The activation times varied depending on the foil material and the time available. Gold was activated for three days; indium for one day; and silver for 14 days. Following exposure the foils were removed and decay counts were measured on the HPGe and the beta detectors in a separate low background room. The counting time was adjusted for each foil material to achieve the equivalent counts of a 50 percent activated foil counted for one hour. The gold was counted of one hour; the indium for 30 minutes; and the silver for 12 hours.

For the HPGe detector, the Genie software was used to subtract the background and compute the area and error. The background was manually subtracted from the total

number of counts for the beta detector. From the resulting thermal activity the thermal flux and associated error were computed.

Limit of Detection

The limit of detection (LOD) is the lowest neutron flux that results in an activity that is statistically different from the background. The limit of detection is defined as the neutron flux associated with three times the standard deviation of the lowest activity divided by area. (22)

To determine the limit of detection for each data set, the activity from thermal neutrons divided by area versus neutron flux was plotted. One-sigma error bars were placed on all data points. The data point corresponding to the lowest neutron flux was used for the LOD. The activity from thermal neutrons divided by area that corresponds to three-sigma error of the data point was identified and its corresponding neutron flux was the limit of detection. Annex C shows these charts.

If the neutron flux that corresponds to the lowest data point is more than three times larger than the calculated limit of detection then a new data point was derived to ensure the LOD was not underestimated. The following procedure was used to develop the new data point. Counts, C_n, are determined using equation 21 where C_t is the number of counts registered by the detector and C_b is the number of background counts.

$$C_n = C_t - C_b \qquad [21]$$

The error associated with counts is determined by adding the resulting errors in quadrature as in equation 22.

$$\sigma_{cn} = \sqrt{\sigma_{ct}^2 + \sigma_{cb}^2} \qquad [22]$$

This procedure adjusts the number of counts and its associated error but keeps all other parameters the same during the calculations, resulting in a new activity divided by area value and its corresponding LOD.

Minimum Area

The minimum foil area required to detect an LOD of 0.5 n/cm^2-sec was determined. For each element the foil size and gamma energy that had the largest number of counts was used. This translated to the least error and smallest limit of detection. The slope of the line generated by the LOD as a function of area was used to define the relationship between activity divided by area and neutron flux,

$$y = x / slope,$$

where y = neutron flux and x = activity divided by area. With this relationship, the known variables determined experimentally and equation 3, the area was scaled to a new LOD of 0.5 n/cm^2-sec. The error in counts is

$$R_\sigma = \sqrt{C}/t,$$

where C is the number of counts and t is the counting time. The LOD is

$$LOD = (3 \times R_\sigma)/area.$$

Using the definition of LOD the new area can be determined. Finally, the LOD was scaled to the target flux of 0.5 n/cm^2-sec. With this new foil area a new rate of activity, R, was determined. Again using equation 3, the new rate of activity and the new flux, a

new area was determined. Equation 23 shows the new relationship for N, the number of radioactive nuclei,

$$N = \frac{area \times N_a \times \rho \times w}{AW}, \qquad [23]$$

where N_a is Avagadro's number, ρ is the density, w is the thickness of the foil, and AW is the atomic weight. When area is solved for in equation 24 the following relationship is found,

$$area = \frac{R_{new} \times AW}{\sigma \times \phi \times N_a \times \rho \times w}. \qquad [24]$$

IV. RESULTS AND ANALYSIS

This chapter consists of three sections. The theoretical section gives the results for the theoretical portion of the thesis while the Laboratory Experiments section gives the results for the experimental portion. The final section, Analysis, ties the results together with the objectives of the thesis.

Theoretical Analyses

This portion of the thesis contains theoretical data for the minimum flux detectable, the minimum time needed to detect a specific flux, and what gaps in coverage exist when all foils are combined into a detection package. All five foils were examined to answer the following three groups of questions.

1. Minimum Neutron Flux:

    a. What is the minimum neutron flux that would produce an activity that could be detected by a HPGe in a high background environment?

    b. What is the minimum neutron flux that would produce an activity that could be detected by a HPGe detector in a low background environment?

    c. What is the minimum neutron flux that would produce an activity that could be detected by a beta detector in a low background environment?

2. Minimum Time to Detect a Neutron Flux:

    a. What is the minimum activation time necessary in a specific neutron flux that would produce an activity that could be detected by a HPGe in a high background environment?

    b. What is the minimum activation time necessary in a specific neutron flux that would produce an activity that could be detected by a HPGe detector in a low background environment?

c. What is the minimum activation time necessary in a specific neutron flux that would produce an activity that could be detected by a beta detector in a low background environment?

3. Detector System Coverage:

a. If the five foils examined were used together in a detector system, would it provide continuous coverage over a 700-day period if the foils were read in a high background with a HPGe detector?

b. If the five foils examined were used together in a detector system, would it provide continuous coverage over a 700-day period if the foils were read in a low background with a HPGe detector?

c. If the five foils examined were used together in a detector system, would it provide continuous coverage over a 700-day period if the foils were read in a low background with a beta detector?

Assumptions

The theoretical section investigated the following foils: silver, gold, indium, europium, and gadolinium. For all of the theoretical calculations, the author assumed all foils were activated in the appropriate flux for two years; and once removed, the foils were counted for one hour in each detector. All foils used were assumed 1 mil thick, elementally pure, and circular with a radius of 5 centimeters.

Minimum Neutron Flux

The following two tables contain the minimum flux required to be detected. All of the reactions required fluxes greater than the target value of 0.5 n/cm^2-sec.

Table 2 shows the minimum detectable flux required by the HPGe detector in both a high and low background environment. When a reaction possessed multiple peaks, the

peak with the lowest flux was used. Gadolinium and $^{108}Ag_m$ required fluxes larger than desired in this thesis. The counting background proved to have a large impact. Counting under the low instead of high background environment reduced the required flux by a factor of six.

Table 3 shows the minimum detectable flux required by the beta detector. All of the foils except gadolinium appeared promising in their ability to detect low fluxes. The beta detector showed more sensitivity in detecting low foil activities.

Table 2 The minimum neutron flux [n/ cm^2-s] required to be detected by a HPGe detector in both high and low background environments

Reaction	**Minimum Flux [n/cm^2-s] Required To Have an Activity Greater than High Background + 3 Standard Deviations**	**Minimum Flux [n/cm^2-s] Required To Have an Activity Greater than Low Background + 3 Standard Deviations**
$^{152}Gd \rightarrow {}^{153}Gd$	26305	1960
$^{158}Gd \rightarrow {}^{159}Gd$	17745	2065
$^{107}Ag \rightarrow {}^{108}Ag_m$	10754	2120
$^{109}Ag \rightarrow {}^{110}Ag_m$	78	17
$^{115}In \rightarrow {}^{116}In_m$	44	15
$^{151}Eu \rightarrow {}^{152}Eu$	20	4
$^{151}Eu \rightarrow {}^{152}Eu_m$	9	2
$^{153}Eu \rightarrow {}^{154}Eu$	118	31
$^{197}Au \rightarrow {}^{198}Au$	58	10

Table 3 The minimum neutron flux [n/ cm^2-s] required to be detected by a beta detector in low background environment

Isotope	**Minimum Flux [n/cm^2-s] Required To Have an Activity Greater than Background + 3 Standard Deviations**
Gd	389
Ag	3
In	2
Eu	1
Au	2

Minimum Time to Detect

Tables 2 and 3 gave the minimum detectable flux. However, this data reveals no timing information. It is not known, when during the theoretical two years of activation the foil's activity would become large enough to be detected above background.

Annex B shows when the signal from each decay first becomes detectable above background at fluxes of 1, 70, 200, and 1000 [n/cm^2-sec]. Gadolinium and $^{108}Ag_m$ do not have the sensitivity required under the fluxes investigated.

Table 4 summarizes the results of Annex B by showing the minimum number of days the isotope must be activated to have an activity high enough to be detected. Table 4 compares the low and high backgrounds for each decay under fluxes of 70 and 200 [n/cm^2-sec]. The consequence of background is obvious. Even with a much higher flux the foils counted in the high background chamber must be activated three to four times longer to detect the activity.

As expected, the beta analysis shows that the higher the flux, the sooner the activity can be detected. Surprisingly, the activities for minimum detection can be attained sooner when counted with the beta detector than with the HPGe detector.

Table 4 The minimum number of days required in a neutron flux to be detected by a HPGe detector in both high and low background environments

Reaction	**Number of days until activity is detectable with a flux of 70 [n/cm^2-s] in a Low Background**	**Number of days until activity is detectable with a flux of 200 [n/cm^2-s] in a Low Background**	**Number of days until activity is detectable with a flux of 200 [n/cm^2-s] in a Low Background**
$^{109}Ag \rightarrow {}^{110}Ag_m$	135	42	368
$^{115}In \rightarrow {}^{116}In_m$	<1	<1	<1
$^{151}Eu \rightarrow {}^{152}Eu$	27	10	130
$^{151}Eu \rightarrow {}^{152}Eu_m$	<1	<1	<1
$^{153}Eu \rightarrow {}^{154}Eu$	157	54	670
$^{197}Au \rightarrow {}^{198}Au$	5	<1	3

Table 5 The minimum number of days required in a neutron flux to be detected by a beta detector in low background environment

Isotope	**Number of days until activity is detectable with a flux of 70 [n/cm^2-s] in a Low Background**	**Number of days until activity is detectable with a flux of 200 [n/cm^2-s] in a Low Background**
Ag	14	5
In	<1	<1
Eu	<1	<1
Au	<1	<1

Detection Timing

This segment examined the performance of the five foils when combined into a detector system over a theoretical 700-day period of activation. Detectable reactions have an activity greater than three standard deviations above background.

The time it takes a foil to reach saturation activity is independent of the neutron flux. Saturation has been reached, in this thesis, when $1-e^{-\lambda t}=99\%$.

At a minimum, the foil detection system required one foil at saturation, to determine the flux, and one foil in the time dependent phase, to ensure an unperturbed neutron source. After 6 hours, $^{116}In_m$ reached saturation so, as long as at least one other foil in the packet had a detectable activity, the system was able to provide information about the neutron source. Table 6 shows the activation time required to achieve saturation for the remaining reactions of interest.

Table 6 The activation time required to achieve saturation

Isotope	**Time Until Saturation**
^{197}Au	18 day
$^{116}In_m$	6 hour
$^{110}Ag_m$	4.5 year
^{152}Eu	90 year
$^{152}Eu_m$	2.6 day
^{154}Eu	57 year

Table 7 and 8 show the number of time dependent detectable foils during the 700-day lifetime of the detector system. The HPGe detector can distinguish between different gamma energies. However, gaps of time exist where there was not a time dependent reaction detectable above background. While these gaps were dependent upon the background, the length of the gaps was exacerbated by the small number of counts that were divided between different energy channels, due to multiple decay schemes, rendering the signal indistinguishable above background. During these times the foil system cannot be used to identify a disturbed neutron source.

Table 7 compares the coverage of the detector system using the HPGe detector under high flux, high background; high flux, low background; and low flux, low background.

In the high flux, high background environment only one time dependent foil could be read above background before day 18. At day 18, ^{198}Au reached saturation and ^{152}Eu was not visible until day 130 leaving an almost four month gap where the detector system could not be used to identify a perturbed neutron source. The detector packet did not possess redundancy of time-dependent activity until more than one year of activation. One reaction, ^{154}Eu, never became visible above background.

In the high flux, low background environment no gaps in coverage surfaced and the only breaks in redundancy occurred early in the activation process. ^{154}Eu became visible on day 54 giving the system three time-dependent foils after less than two months of activation.

In the low flux, low background environment some early gaps in coverage appeared but after one month of activation the foil packets gave constant coverage. Redundancy occurred after day 135.

Table 8 shows similar results regardless of flux for the beta detector. Throughout the test period there was always redundancy of time-dependent foils and the only difference was the time silver appeared above background.

HPGe can be used to differentiate between different isotopes. In essence an activated europium foil appears as three foils for the gamma detector. Because the beta detector does not distinguish between energies, the activation curve for europium appeared quickly and was always time dependent due to the influence of ^{152}Eu, $^{152}Eu_m$, and ^{154}Eu, all with very different half-lives.

Table 7 The number of time dependent foils available to be read by the HPGe detector during a 700 day monitoring period in high and low background environments.

High Background 200 [n/cm^2-sec]		**Low Background 200 [n/cm^2-sec]**		**Low Background 70 [n/cm^2-sec]**	
days	**# of time dependent foils**	**days**	**# of time dependent foils**	**days**	**# of time dependent foils**
0-3	1	0-3	2	0-3	1
3-18	1	3-10	1	3-5	0
18-130	0	10-18	2	5-18	1
130-368	1	18-42	1	18-27	0
368-700	2	42-54	2	27-135	1
		54-700	3	135-157	2
				157-700	3

Table 8 The number of time dependent foils available to be read by the beta detector during a 700 day monitoring period in low background environment.

Low Background 200 [n/cm^2-sec]		**Low Background 70 [n/cm^2-sec]**	
days	**# of time dependent foils**	**days**	**# of time dependent foils**
0-5	2	0-14	2
5-18	3	14-18	3
18-700	2	18-700	2

Laboratory Experiments

This is the experimental portion of the thesis and it contains the neutron flux limit of detection for the three foils tested and the minimum foil size required to detect the target flux. The test results were used to answer the following questions:

1. For each key gamma of each foil investigated, what are the limits of detection for the HPGe detector?

2. For each foil investigated, what are the limits of detection for the beta detector?

3. Using the same parameters determined by the limits of detection for the HPGe detector, what is the minimum area required by each key gamma of each foil investigated to detect the target flux?

4. Using the same parameters determined by the limits of detection for the beta detector, what is the minimum area required by each foil investigated to detect the target flux?

Assumptions

Gold, indium, and silver were used in the experiments. The foils were assumed elementally pure. Foils of two different areas were used, 0.79 cm^2 and 12.9 cm^2. Counting time adjustments were made so all foils targeted the equivalent counts of a 50 percent activated foil. All foils were placed in the same flux. After activation the foils were counted using the Canberra Model GC10021 High Purity Germanium detector and the Canberra Model 2400 Alpha/Beta detector system. All counting was done in the lowest background environments possible and the standard count was for one hour.

Limit of Detection

Many factors affect a system's ability to detect a low neutron flux including but not limited to: the noise in the electronics, the background, the size of the foil, and the

efficiency of the detector. The LOD is the lowest neutron flux detectable with statistical reliability.

The determination of the LOD is based solely on the error of the activity as a function of area. The error in the area is constant. The error in activity is heavily dependent upon the number of counts; consequently, the larger the area, the lower the LOD. However, the detector limits the foil's size. Increasingly larger size results in a diminished efficiency. Another factor that affects the number of gamma counts is the number of competing decay chains. If competing decay chains produce gammas at many different energies, the already small signal becomes diluted and masked by the noise. Table 9 shows the LOD from gold and indium using the HPGe detector while Table 10 shows the LOD from gold, indium, and silver using the beta detector.

Gold has ideal characteristics for this problem. Gold possesses one dominant decay scheme, which produces a single mono-energetic gamma ray for every beta particle. This results in an easy to compute relationship between gamma and beta counts with no dilution of the gamma signal. The one-mil thick gold foil averaged 54 percent activation. The foils were counted for one hour by both detectors. Gold produced the lowest gamma LOD, 8.5 n/cm^2-sec.

Counting times were adjusted for indium due to its short half-life. The calculations were adjusted for the two-mil thick indium foil used. Indium was 100 percent activated and counted for 30 minutes. This produced the same number of counts as if a 50 percent activated foil was counted for one hour. The conditions compared to gold except for indium's multiple decay pathways. Indium produced three major gamma peaks at 416 keV, 1097 keV, and 1293 keV. Despite a larger cross-section than gold the LODs for indium were significantly higher because of the reduced counts for each peak. The gamma peak, 1293 keV had the best LOD for indium at 19 n/cm^2-sec.

The dilution of counts due to multiple gamma peaks significantly affected the performance of the HPGe detector with the silver foils. The silver foil's dominant peak, 657 keV could not be determined. Consequently, only the beta detector was used for counting silver. Silver was selected because of its large half-life. The five-mil silver foils were counted for 12 hours, producing the same number of counts that would have been detected if the foil had been removed from the flux on day 220 and had been 46 percent activated. Even though the counts were equivalent, the statistics were not. A 12-hour background overwhelmed the small number of counts which would not occur with a one-hour background. The dominance of the background counts caused an unusually high LOD. If the silver foil had been activated for 220 days, one would expect an LOD in the range of 36 n/cm^2-sec for the small area and 26 n/cm^2-sec for the large area, which is in line with the values of the other two foils.

Table 9 The limit of detection for gold and indium foils using the HPGe detector

	Small Area [0.8 cm^2]	**Large Area [12.9 cm^2]**
Gold	63 n/cm^2-sec	8.5 n/cm^2-sec
Indium 416 keV	150 n/cm^2-sec	40 n/cm^2-sec
Indium 1097 keV	130 n/cm^2-sec	22 n/cm^2-sec
Indium 1293 keV	110 n/cm^2-sec	19 n/cm^2-sec

Table 10 The limit of detection for gold, indium and silver foils using the beta detector

	Small Area [0.8 cm^2]	**Large Area [12.9 cm^2]**
Gold	32 n/cm^2-sec	22 n/cm^2-sec
Indium	33 n/cm^2-sec	23 n/cm^2-sec
Silver	150 n/cm^2-sec	99 n/cm^2-sec

Minimum Area to Detect

One approach to improve the limit of detection is to increase the number of target atoms for the neutrons to activate. Assuming the efficiency and all other factors remain the same as in the previous section, Table 11 shows the minimum area of a foil required to detect a flux of 0.5 n/cm^2-sec. The 1293 keV gamma peak statistics were used for the indium calculation. Only beta measurements were conducted on silver.

Table 11 The minimum foil area required to detect the target flux assuming all detector parameters remain the same as experimentally determined for smaller foils

Element	Minimum Area for HPGe Detector [cm^2]	Minimum Area for Beta Detector [cm^2]
Gold	690	800
Indium	800	890
Silver	N/A	1600

Analysis

The purpose of this project was to investigate, using activation theory and experiments, the feasibility of an activation foil detection system in a low neutron flux and to determine if a neutron signal, just at the limit of detection, could be detected with statistical reliability.

In the theoretical section the author determined the minimum detectable flux with a one-mil thick, elementally pure, circular foil with a radius of 5 centimeters. The foil size was chosen because it was the largest size that was compatible with the detectors used in this thesis. The experimental section determined the limit of detection for three of the five foils investigated in the theoretical section. For both sections, the minimum flux detectable was larger than the target flux of 0.5 n/cm^2-sec.

If the target flux cannot be detected by the methods used in either the theoretical or experimental portions, the question becomes, what adjustments are required to lower the limit of detection so the target flux can be reliably detected? Some possible answers follow.

As equation 3 showed, activity is proportional to the number of target atoms. Therefore, to increase activity, the foil can be made either bigger or thicker in order to increase the number of target atoms. Unfortunately, problems exist with these solutions. Calculations found in Table 11 indicates that under the measured experimental efficiencies found in the experimental section the foils must possess an area on the order of 625 cm^2 to measure the target flux. These foils are too big to use detectors similar to the ones used in this thesis. Activation theory works only with thin foils because it assumes that all target atoms have an equal chance of interacting with the flux. With increasing thickness less neutrons will reach atoms on the interior of the foil due to absorption and scattering. Additionally, the radiation from interior activated atoms can be absorbed or scattered by the target atoms on the outside.

Another approach to lowering the limit of detection is to obtain larger counts. The detector will discern additional counts if the efficiency, solid angle, or counting time is increased. Because counts drive the limit of detection, resolution can be sacrificed for enhanced efficiency. The beta detector used in the experimental section could not distinguish between energies but had limits of detection lower than the HPGe for smaller counts. The greater resolution of the HPGe divided the energies up to distinguish one from another but due to the low count the signal became statistically indistinguishable from the background thus increasing the limits of detection.

A HPGe well detector or 4π gas flow proportional counter could be used to increase the efficiency but the maximum sample size is too small. A solution to this size limitation might be to use a sodium iodide (NaI(Tl)) detector. The crystals for NaI(Tl)

detectors can be made large and have good efficiency. A recommended detector size is a 13 inch diameter by 5 inch thick NaI(Tl) detector. (23) However, this solution introduces a new problem; increased detector size results in increased background counts.

Measurements conducted in this thesis were done in low background environments, with no active suppression. However, if the background counts were further reduced, the foils could be counted longer without statistical penalties applied for the increased counts associated with background.

The final option to get more counts is to optimize the foil selection. Of the foils examined in this thesis only two, europium and gadolinium, were chosen specifically for this project. The other foils, gold, silver, and indium, were chosen because of the materials' availability for testing and previous work done on gold and indium. A better selection of foils with higher cross sections and single decay chains could help make this project possible.

This problem is one of optimization. If the right detector, background, and foil combination is combined the target flux may be detectable.

V. RECOMMENDATIONS AND CONCLUSION

Conclusion

The driving force behind this thesis is national security and the question of how can the United States ensure countries abide by their treaties concerning SNM. Two foundational questions are:

1- Is a system of activation foils for detecting a low flux of neutrons from SNM feasible?

2- Does this concept warrant further investigation?

The answer to the former question is a resounding maybe. The theoretical and laboratory experiments performed in this thesis were a factor of 4 to 6 times larger than the target flux. However, many courses of action exist for further study to fine tune the system and lower the limit of detection.

The key to the potential success of this project is optimization. There are many characteristics of the foils and counting that can be manipulated to produce enhanced sensitivity including: larger foil size, anticoincidence techniques to reduce background, developing detectors and configurations to increase efficiency, and an improved selection of foils.

Recommendations for Future Work

Because this area of research warrants further investigation, the following recommendations are offered to focus further research. This thesis looked at individual foils and a foil detector system. The foil detector system examined the effects of the counting background on the coverage of the detector system. The Individual Foils portion investigated the theoretical minimum detectable neutron flux, the experimental limits of detection and minimum area required to determine the target flux were determined for three of the five foils examined. All of the methods examined failed to

have the sensitivity to detect the target flux. However, the research opened the following areas for discussion.

Detector System

A detection system can be designed to get more counts from the activated foil. One example of a system that can be developed is a simulated 4π counter using two HPGe detectors. The HPGe detectors are arranged face to face with the activated foil placed in between. This configuration will result in doubling the counts detected, both from the activated foil and from background. Even with the additional background counts, it is estimated that the limit of detection can be reduced by 30 percent using this configuration.

Both equipment configurations have intrinsic error that will need to be addressed. Figure 13 shows the two HPGe detectors with separate electronics for each detector. This system has added expense due to the duplicate electronics but the main difficulty is with energy matching. Each computer has a slightly different division for the MCA energy bins. The error appears when the data from one detector is added to the data from another detector. The result is that the same energy may be deposited in slightly different bins depending on how it is divided up. This results in a shift to the energy declaration of each bin. This result can be significant over an energy range greater than 100 keV. However, if the energy range is shortened to 20 to 50 keV the end result of merging the data should not be significant.

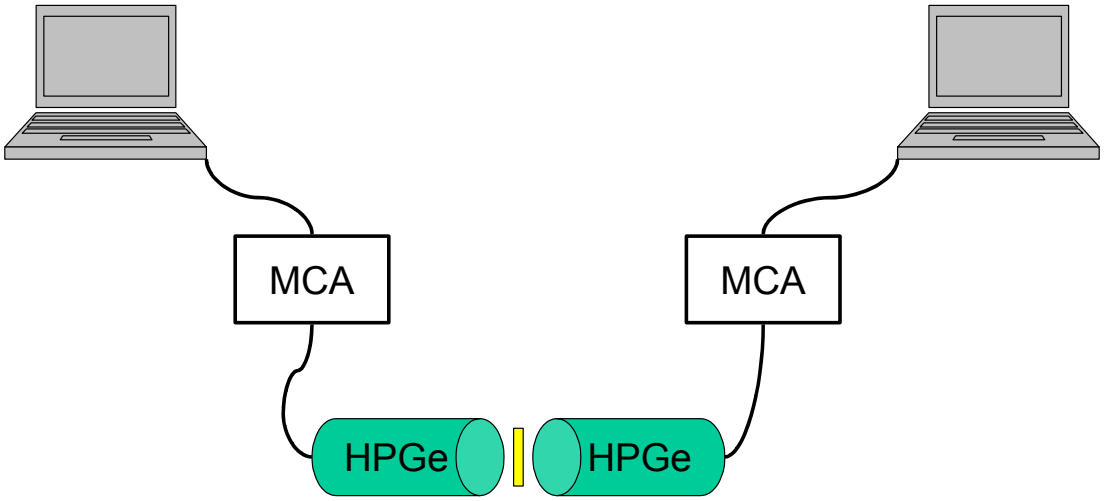

Figure 13 A simulated 4π counter using two HPGe detectors and separate electronics

Another approach is shown in Figure 14 where the two detectors are linked before the signal reaches the MCA. This system is less expensive because it uses less equipment and does not have the energy-matching problem. However, if each detector produced a pulse from the foil that reached the linking electronics at the same instant the pulse would be added together producing a peak that has twice the energy of the detected gamma. A predicament arises upon deciding if the coincidence pulses should be counted. If they are not counted then information is not used. However, if the coincidence peaks are counted, how should they be counted? Is each pulse in the coincidence peak to be counted twice? Can all of the pulses in the coincidence peak be attributed to coincidence? How will this influence the statistics?

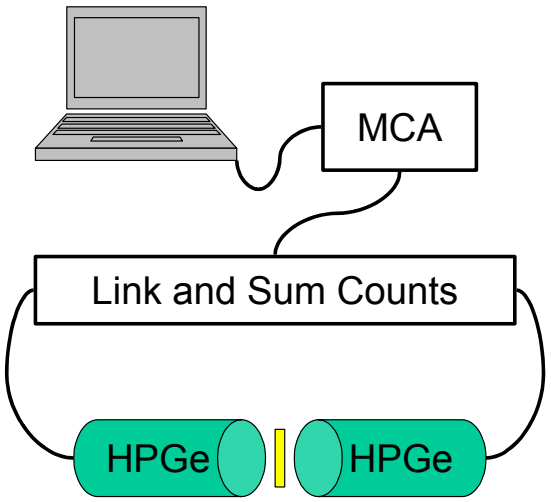

Figure 14 A simulated 4π counter using two HPGe detectors and linked electronics

Neutron Spectrum

Several unsuccessful attempts were made to get a neutron energy spectrum from an actual nuclear weapon in its storage container. No information was made available to the author; so all work was done during this thesis was with thermal neutrons. All neutrons were assumed thermal for the theoretical calculations. During the laboratory portion of this thesis, the energy of the neutrons from the PuBe source was reduced by passing them through 13.5 centimeters of paraffin before the neutrons reached the activating foils. To further ensure all foil activities were a result of thermal neutrons, neutrons were thermalized by the use of cadmium covers.

An unclassified model of the neutron spectrum as the neutrons pass from the hollow plutonium pit through the remainder of the physics package and container is needed. An accurate depiction of the neutron spectrum at the surface of the weapon container would

allow for further optimizing of the detection system and would ensure that the appropriate neutron source is used during laboratory experiments.

To determine the neutron spectrum, modeling codes could be used. Once the result from the models was determined they could be compared to a real spectrum to determine which model to use for future research.

Higher Flux

Another method for getting higher counts is to have an activation foil with a higher activity. Equation 3 shows that activation is proportional to the neutron flux. Positioning the activation foils closer to the neutron source can increase the neutron flux.

One possible method to increase the neutron flux is to incorporate the activation foils into the shipping container. The activation foils can be an integral part of the shipping container and can be read after the SNM is removed or the activation foils can be on a removable sticker placed on the inside of the shipping container. The foils would be placed so they can detect if the lid has been opened.

A second method is to redesign the nuclear weapon or SNM storage containers with a small portal in the storage container wall. As shown in Figure 15, the activation foils can be inserted into the portal, positioning them inside the storage container wall and closer to the neutron source. The portal could be secured with a plug to reduce background neutrons and discourage unauthorized tampering of the activation foils. This method would also reduce the variability of the neutron spectrum due to variations of the placement of the detector on the storage container. The SNM and its container are nonhomogenous and slight variations in the detector placement may have a great influence on the ability to measure and accuracy of the activation foils being used as a monitoring system. If care is taken and the portal is positioned consistently in each

storage container wall, the neutron spectrum could be comparable from container to container.

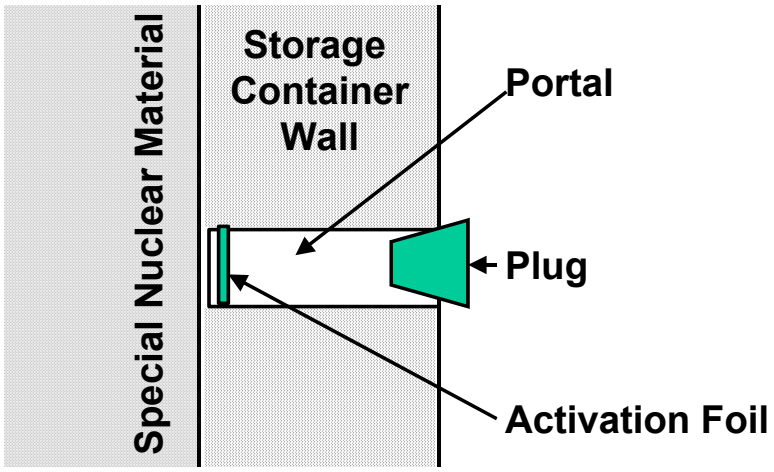

Figure 15 A portal for the positioning of activation foils inside the SNM storage container wall.

Annex A. - Isotope Information

This annex lists the basic information for the isotopes of interest in Table 12 and key gamma information in Table 13.

Table 12 Key Isotope Information

Isotope	Natural Concentration [percent] (18)	Absorption Cross Section for Thermal Neutrons (.0253 eV) [barn] (18)	Product Isotope (19)	Half Life (18)	Key Decay Products Gamma [keV] (24)	Decay Products Beta [MeV] (18)
Gd						
Gd-152	0.2	700	Gd-153	241.6 d	97.4, 103.2	-------
Gd-158	24.8	2.4	Gd-159	18.56 h	363.54	0.96
Gd-160	21.8	1	Gd-161	3.66 m	360.9, 314.9, 102.3	1.56
Gd-154	2.18	60	Gd-155	stable	-------	-------
Gd-155	14.8	61000	Gd-156	stable	-------	-------
Gd-156	20.47	2	Gd-157	stable	-------	-------
Gd-157	15.65	255000	Gd-158	stable	-------	-------
Ag						
107-Ag	51.83	38.62	108m-Ag	130 y	433.92, 614.27, 722.90	-------
107-Ag	51.83	36.35	108-Ag	2.39 m	433.95, 618.85, 632.98	1.65
109-Ag	48.17	3.89	110-Ag	24.6 s	657.8	2.981
109-Ag	48.17	91.4	110m-Ag	249.8 d	657.74, 763.93, 884.67, 937.48, 1384.27	0.087, 0.530

Table 12 Key Isotope Information - Continued

Isotope	Natural Concentration [percent] (18)	Absorption Cross Section for Thermal Neutrons (.0253 eV) [barn] (18)	Product Isotope (19)	Half Life (18)	Key Decay Products Gamma [keV] (24)	Decay Products Beta [MeV] (18)
In						
113-In	4.3	56	114m-In	49.51 d	190.27, 558.43, 725.24	-------
113-In	4.3	2	114-In	72 s	1299.9	1.984
115-In	95.7	162	116m-In	54.2 m	416.88, 1097.23, 1293.49,	1
115-In	95.7	42	116-In	14.1 s	1293.6, 463.3	3.3
Eu						
151-Eu	47.9	5900	Eu-152	13.54 y	121.78, 244.70, 344.27, 788.87, 964.04, 1085.83, 1112.09, 1408.02	0.699
151-Eu	47.9	3300	Eu-152m	9.29 h	121.78, 841.54, 963.34	1.86
153-Eu	52.2	320	Eu-154	8.593 y	122.90, 723.31, 873.25, 996.37, 1004.87, 1274.50	0.58, 0.27
Au						
197-Au	100	98.7	198-Au	2.695 d	411.79	0.962

Table 13 Key Gammas

153-Gd

Energy [keV]	Error +/-	Relative Intensity	Error +/-	HPGe Abs Efficiency
97.43	0.01	100.00	5.00	3.672E-03
103.18	0.00	73.50	1.00	3.996E-03

159-Gd

Energy [keV]	Error +/-	Relative Intensity	Error +/-	HPGe Abs Efficiency
363.51	0.01	100.00	5.00	4.320E-03

108m-Ag

Energy [keV]	Error +/-	Relative Intensity	Error +/-	HPGe Abs Efficiency
433.92	0.04	100.00	5.00	3.888E-03
614.27	0.05	100.00	5.00	3.024E-03
722.90	0.05	100.00	5.00	2.808E-03

110m-Ag

Energy [keV]	Error +/-	Relative Intensity	Error +/-	HPGe Abs Efficiency
657.74	0.02	100.00	5.00	2.916E-03
763.93	0.02	23.99	1.25	2.700E-03
884.67	0.02	77.87	3.95	2.484E-03
937.48	0.02	37.40	1.91	2.376E-03
1384.27	0.03	26.79	1.41	1.944E-03

116m-In

Energy [keV]	Error +/-	Relative Intensity	Error +/-	HPGe Abs Efficiency
416.88	0.03	29.37	2.00	3.996E-03
1097.23	0.04	67.91	3.20	2.160E-03
1293.49	0.05	100.00	2.00	1.944E-03

Table 13 Key Gammas - Continued

152-Eu

Energy [keV]	Error +/-	Relative Intensity	Error +/-	HPGe Abs Efficiency
121.78	0.01	100.00	5.00	4.968E-03
244.70	0.01	27.90	1.30	5.508E-03
344.27	0.01	97.90	4.50	4.536E-03
778.87	0.02	48.00	2.00	2.592E-03
964.04	0.02	53.50	0.23	2.376E-03
1085.83	0.02	38.85	1.70	2.160E-03
1112.09	0.02	49.75	2.20	2.160E-03
1408.02	0.03	78.10	3.40	1.836E-03

152m-Eu

Energy [keV]	Error +/-	Relative Intensity	Error +/-	HPGe Abs Efficiency
121.78	0.01	50.66	2.00	4.968E-03
841.54	0.02	100.00	5.00	2.484E-03
963.34	0.03	82.40	8.00	2.376E-03

154-Eu

Energy [keV]	Error +/-	Relative Intensity	Error +/-	HPGe Abs Efficiency
122.90	0.10	100.00	5.00	4.968E-03
723.31	0.10	54.30	3.00	2.808E-03
873.25	0.11	31.90	1.80	2.484E-03
996.37	0.10	30.26	1.80	2.268E-03
1004.87	0.10	50.49	3.00	2.268E-03
1274.50	0.12	95.00	5.80	2.052E-03

198-Au

Energy [keV]	Error +/-	Relative Intensity	Error +/-	HPGe Abs Efficiency
411.79	0.01	100.00	5.00	3.996E-03

Annex B. - Minimum Time to Detect

This annex lists when the foil activity is initially strong enough to be detected above background. The foils were exposed to thermal neutron fluxes of 1, 70, 200, and 1000 n/cm^2-sec. "N/A" was used to identify those reactions that did not have an adequate activity to be detected above the background after two years. Table 14 and Table 15 were developed using the HPGe detector in a low background and high background environment respectively. Table 16 was developed using the beta detector in a low background environment.

Table 14 Gamma Time of Appearance for Low Background

Isotope	When Flux = 1 [n/cm^2-s] Time When Activity is Greater Than Low Background + 3 Sigma	When Flux = 70 [n/cm^2-s] Time When Activity is Greater Than Low Background + 3 Sigma	When Flux = 200 [n/cm^2-s] Time When Activity is Greater Than Low Background + 3 Sigma	When Flux = 1000 [n/cm^2-s] Time When Activity is Greater Than Low Background + 3 Sigma
Gd				
$^{152}Gd \rightarrow {}^{153}Gd$				
97 keV	N/A	N/A	N/A	N/A
103 keV	N/A	N/A	N/A	N/A
$^{158}Gd \rightarrow {}^{159}Gd$				
363 keV	N/A	N/A	N/A	N/A
Ag				
$^{107}Ag \rightarrow {}^{108}Ag_m$				
433 keV	N/A	N/A	N/A	N/A
614 keV	N/A	N/A	N/A	N/A
722 keV	N/A	N/A	N/A	N/A
$^{109}Ag \rightarrow {}^{110}Ag_m$				
657 keV	N/A	95 day	30 day	6 day
763 keV	N/A	N/A	148 day	25 day
884 keV	N/A	213 day	61 day	12 day
937 keV	N/A	293 day	78 day	14 day
1384 keV	N/A	337 day	86 day	16 day

Table 14 Gamma Time of Appearance for Low Background - Continued

Isotope	When Flux = 1 [n/cm^2-s] Time When Activity is Greater Than Low Background + 3 Sigma	When Flux = 70 [n/cm^2-s] Time When Activity is Greater Than Low Background + 3 Sigma	When Flux = 200 [n/cm^2-s] Time When Activity is Greater Than Low Background + 3 Sigma	When Flux = 1000 [n/cm^2-s] Time When Activity is Greater Than Low Background + 3 Sigma
In				
$^{115}In \rightarrow {}^{116}In_m$				
1293 KeV	30 hour	26 min	8 min	2 min
1097 keV	22 hour	19 min	6 min	1 min
416 keV	N/A	N/A	52 min	8 min
Eu				
$^{151}Eu \rightarrow {}^{152}Eu$				
121 keV	N/A	62 day	21 day	4 day
244 keV	N/A	372 day	128 day	26 day
344 keV	N/A	38 day	14 day	3 day
778 keV	N/A	52 day	18 day	4 day
964 keV	N/A	93 day	32 day	6 day
1085 keV	N/A	98 day	34 day	7 day
1112 keV	N/A	59 day	21 day	4 day
1408 keV	N/A	32 day	11 day	2 day
$^{151}Eu \rightarrow {}^{152}Eu_m$				
121 keV	32 hour	27 min	9 min	2 min
841 keV	22 hour	20 min	7 min	1 min
963 keV	49 hour	42 min	15 min	3 min
$^{153}Eu \rightarrow {}^{154}Eu$				
122 keV	N/A	N/A	339 day	66 day
723 keV	N/A	N/A	463 day	89 day
873 keV	N/A	N/A	307 day	60 day
996 keV	N/A	N/A	324 day	63 day
1004 keV	N/A	N/A	385 day	74 day
1274 keV	N/A	303 day	103 day	20 day
Au				
$^{197}Au \rightarrow {}^{198}Au$				
411 keV	41 day	14 hr	5 hr	55 min

Table 15 Gamma Time of Appearance for High Background

Isotope	When Flux = 1 [n/cm^2-s] Time When Activity is Greater Than High Background + 3 Sigma	When Flux = 70 [n/cm^2-s] Time When Activity is Greater Than High Background + 3 Sigma	When Flux = 200 [n/cm^2-s] Time When Activity is Greater Than High Background + 3 Sigma	When Flux = 1000 [n/cm^2-s] Time When Activity is Greater Than High Background + 3 Sigma
Gd				
$^{152}Gd \rightarrow {}^{153}Gd$				
97 keV	N/A	N/A	N/A	N/A
103 keV	N/A	N/A	N/A	N/A
$^{158}Gd \rightarrow {}^{159}Gd$				
363 keV	N/A	N/A	N/A	N/A
Ag				
$^{107}Ag \rightarrow {}^{108}Ag_m$				
433 keV	N/A	N/A	N/A	N/A
614 keV	N/A	N/A	N/A	N/A
722 keV	N/A	N/A	N/A	N/A
$^{109}Ag \rightarrow {}^{110}Ag_m$				
657 keV	N/A	N/A	178 day	29 day
763 keV	N/A	N/A	N/A	123 day
884 keV	N/A	N/A	196 day	32 day
937 keV	N/A	N/A	424 day	54 day
1384 keV	N/A	N/A	265 day	40 day
In				
$^{115}In \rightarrow {}^{116}In_m$				
1293 KeV	2.9 day	1 hr	19 min	4 min
1097 keV	N/A	N/A	37 min	6 min
416 keV	N/A	N/A	N/A	1 min

Table 15 Gamma Time of Appearance for High Background - Continued

Isotope	When Flux = 1 [n/cm^2-s] Time When Activity is Greater Than High Background + 3 Sigma	When Flux = 70 [n/cm^2-s] Time When Activity is Greater Than High Background + 3 Sigma	When Flux = 200 [n/cm^2-s] Time When Activity is Greater Than High Background + 3 Sigma	When Flux = 1000 [n/cm^2-s] Time When Activity is Greater Than High Background + 3 Sigma
Eu				
$^{151}Eu \rightarrow {}^{152}Eu$				
121 keV	N/A	N/A	539 day	105 day
244 keV	N/A	N/A	N/A	210 day
344 keV	N/A	549 day	187 day	37 day
778 keV	N/A	354 day	122 day	24 day
964 keV	N/A	414 day	142 day	28 day
1085 keV	N/A	323 day	111 day	22 day
1112 keV	N/A	245 day	85 day	17 day
1408 keV	N/A	194 day	67 day	14 day
$^{151}Eu \rightarrow {}^{152}Eu_m$				
121 keV	61 day	21 hr	4 hr	5 min
841 keV	6 day	2 hr	33 min	7 min
963 keV	N/A	N/A	21 hr	2 hr
$^{153}Eu \rightarrow {}^{154}Eu$				
122 keV	N/A	N/A	N/A	N/A
723 keV	N/A	N/A	N/A	308 day
873 keV	N/A	N/A	N/A	356 day
996 keV	N/A	N/A	N/A	308 day
1004 keV	N/A	N/A	N/A	220 day
1274 keV	N/A	N/A	N/A	80 day
Au				
$^{197}Au \rightarrow {}^{198}Au$				
411 keV	490 day	7 day	1 day	6 hr

Table 16 Beta Time of Appearance

Isotope	When Flux = 1 [n/cm^2-s] Time when Activity is greater than Background + 3 sigma	When Flux = 70 [n/cm^2-s] Time when Activity is greater than Background + 3 sigma	When Flux = 200 [n/cm^2-s] Time when Activity is greater than Background + 3 sigma	When Flux = 1000 [n/cm^2-s] Time when Activity is greater than Background + 3 sigma
Gd	N/A	N/A	N/A	N/A
Ag	More than 2 years	14 day	5 day	1 day
In	2 hour	2 min	1 min	1 min
Eu	5 hour	4 min	2 min	1 min
Au	5 day	98 min	34 min	7 min

Annex C. - Limit of Detection

This annex holds the charts that were used to determine the limit of detection for gold, indium, and silver. The error bars are one sigma to the left and right of the data point. The gold charts designate area as Small/Small, small bare and cadmium-covered foil, Large/Small, large bare and small cadmium-covered foil, and Large/Large, large bare and cadmium-covered foil. For the other two foils "small", small bare and cadmium-covered foil, and "large", large bare and cadmium-covered foil, were used to describe the area.

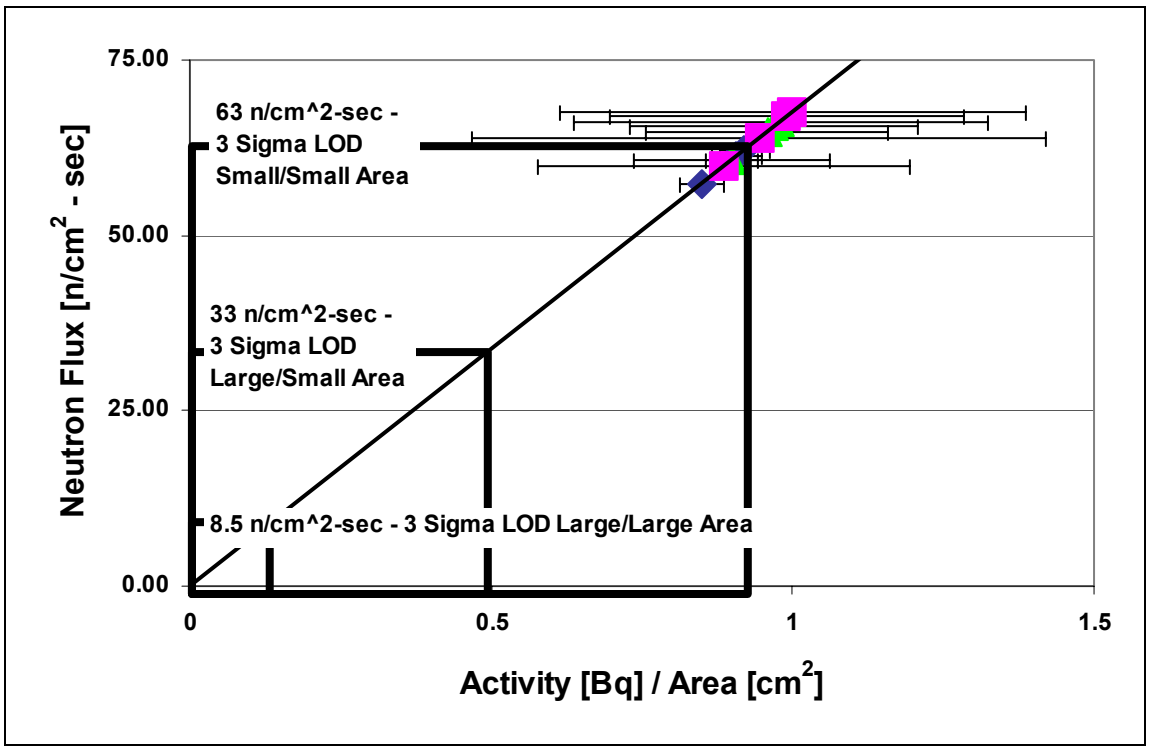

Figure 16 Gamma LOD for Gold

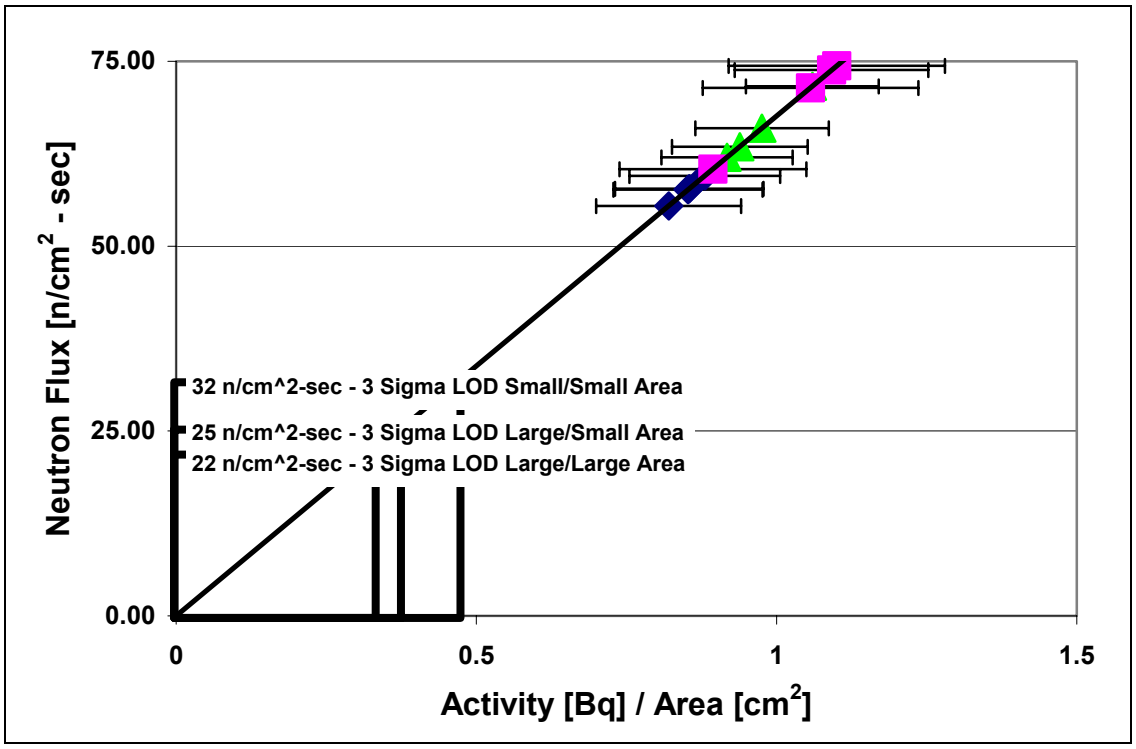

Figure 17 Beta LOD for Gold

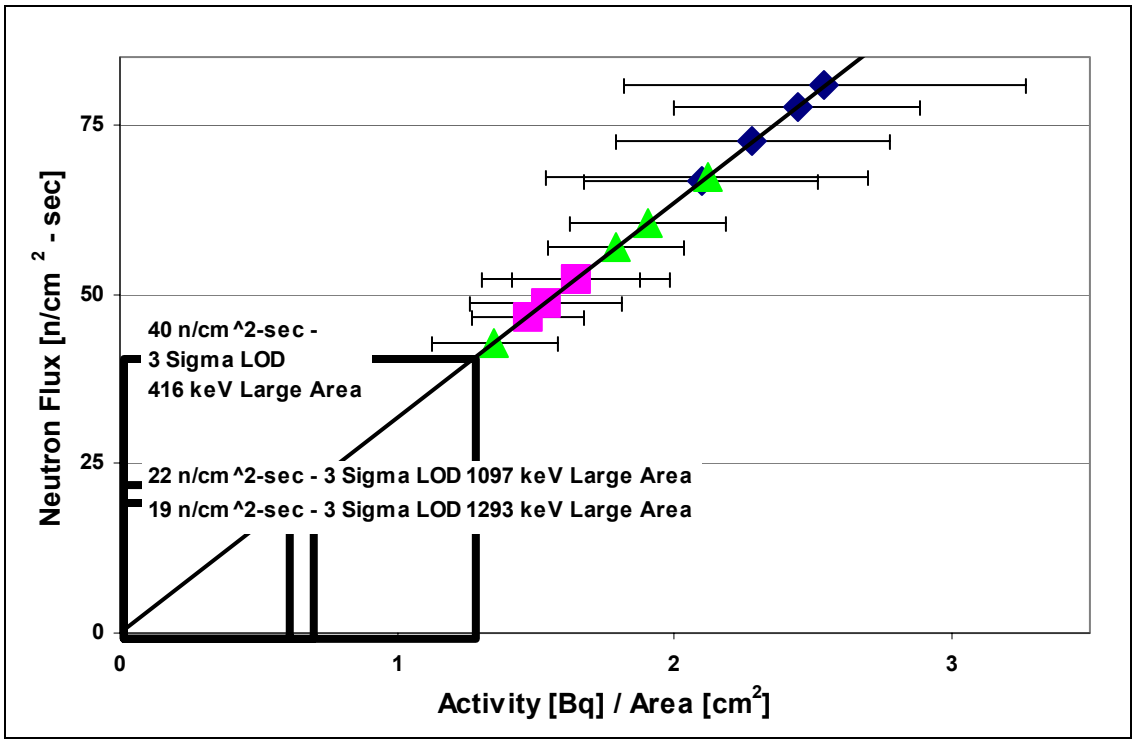

Figure 18 Gamma Large Area LOD for Indium

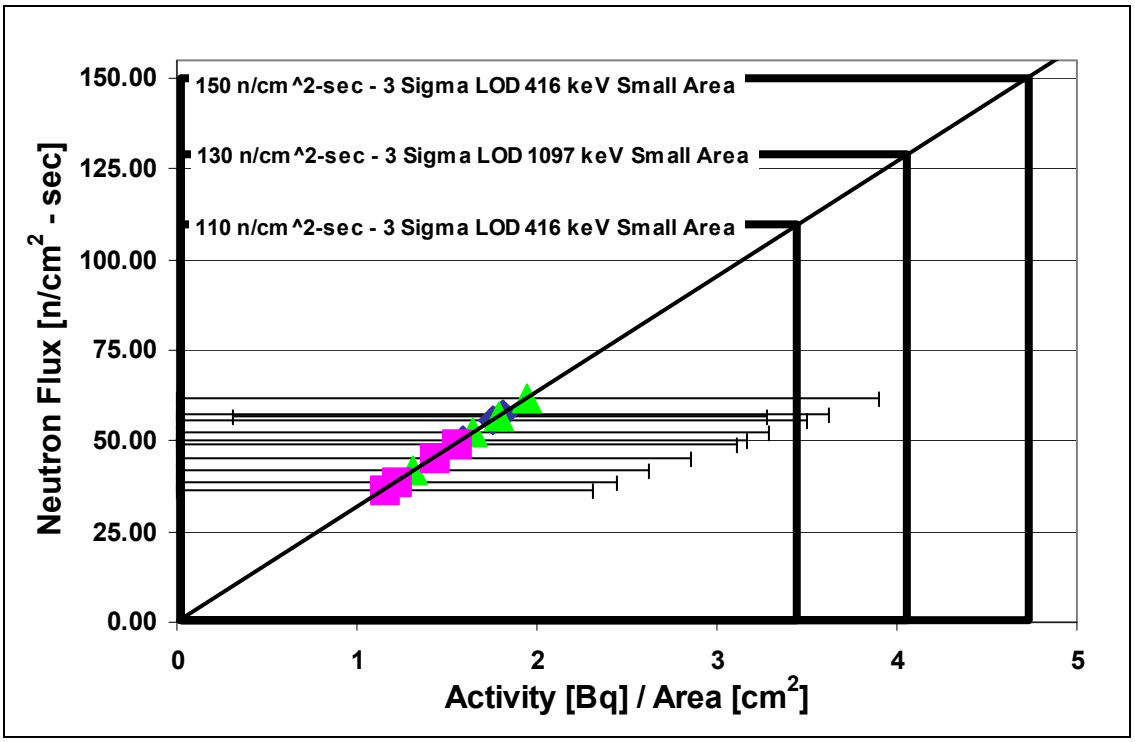

Figure 19 Gamma Small Area LOD for Indium

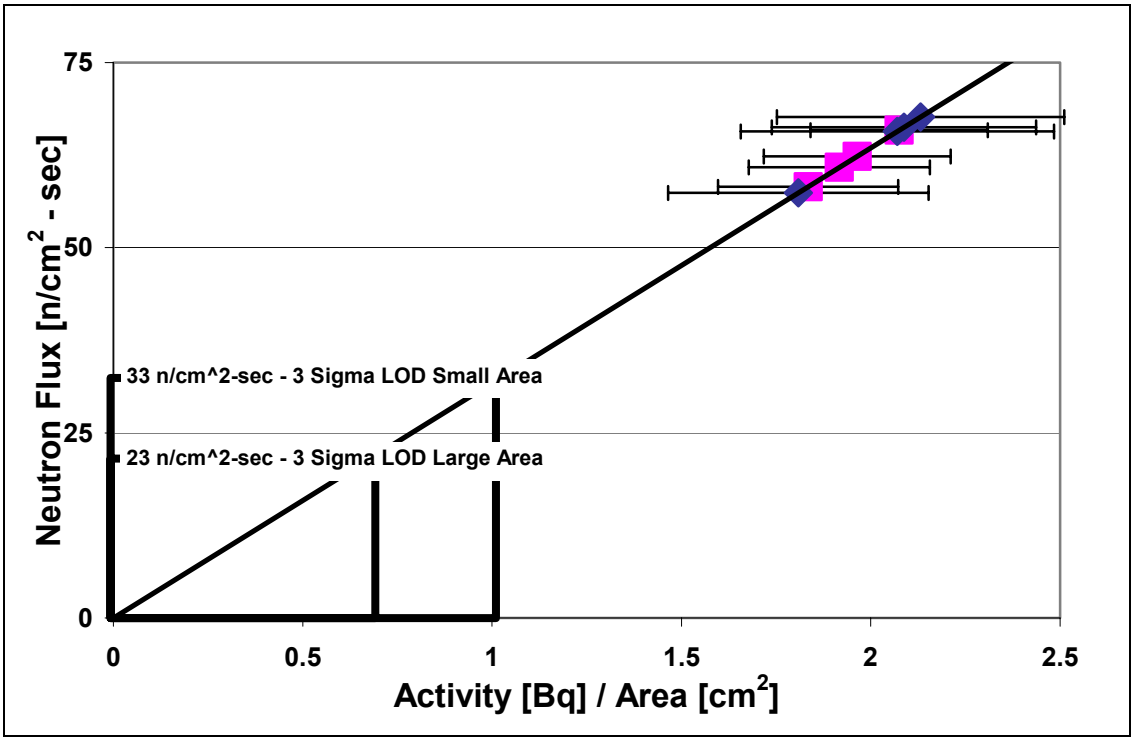

Figure 20 Beta LOD for Indium

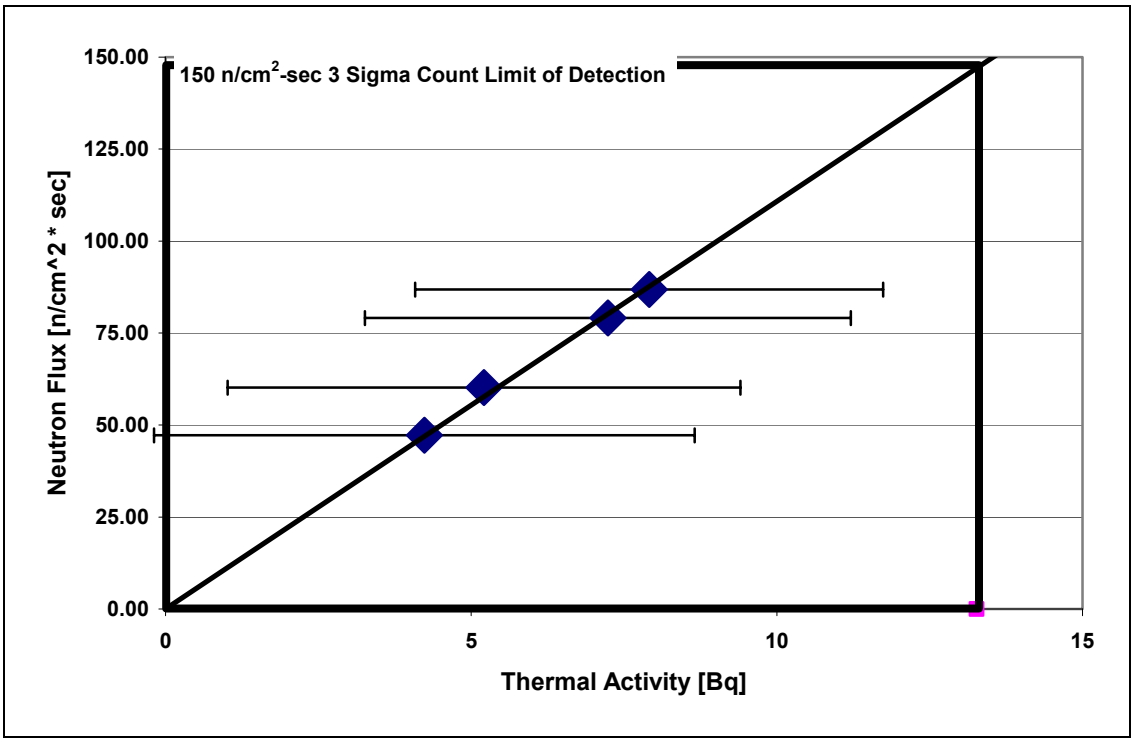

Figure 21 Beta LOD for Indium

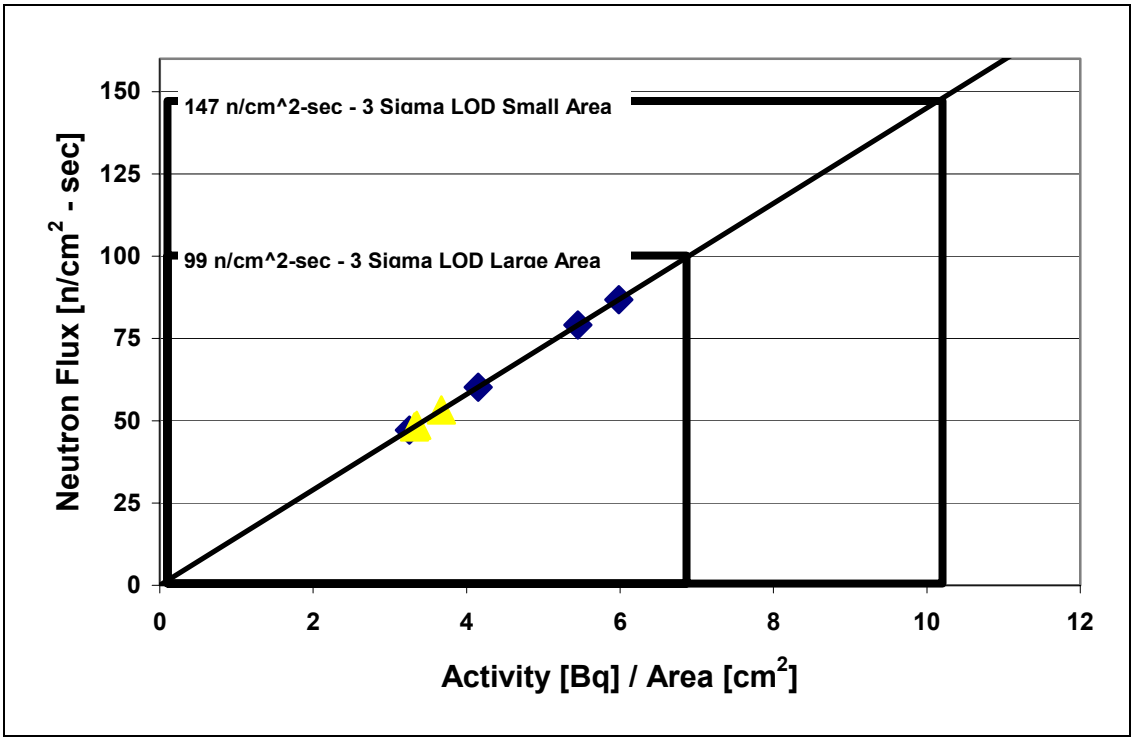

Figure 22 Beta LOD for Silver

Annex D. - Decay Schemes

This annex shows the decay schemes of the isotopes of interest in this thesis. The diagrams are a statistical representation. If there are two possible pathways the probability is shown as a percentage. The isotopes shown in gray are the stable isotopes. If there is more than one reaction the separate reactions are marked with a ① or a ② for reference.

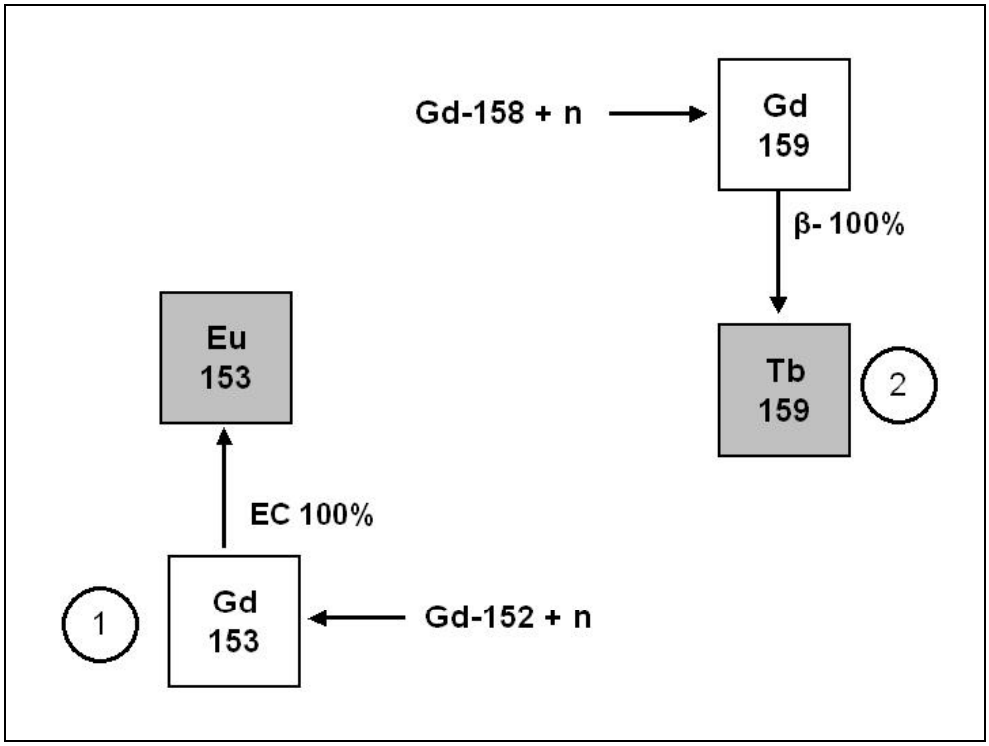

Figure 23 Decay Scheme for Gd-153 and Gd-159

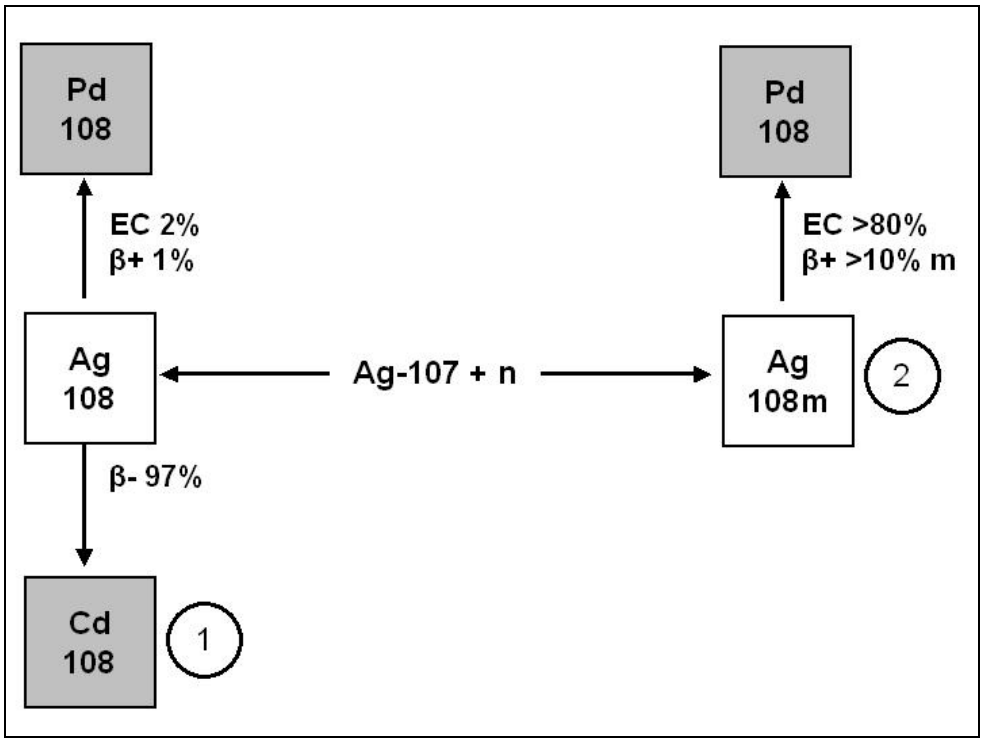

Figure 24 Decay Scheme for Ag-108 and Ag-108m

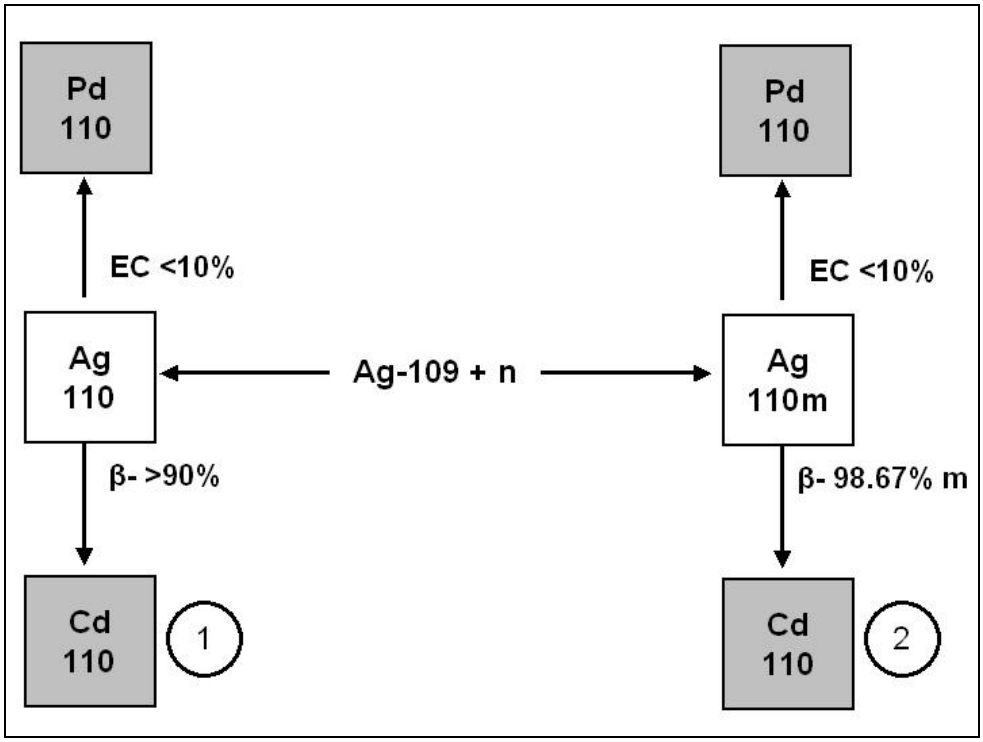

Figure 25 Decay Scheme for Ag-110 and Ag-110m

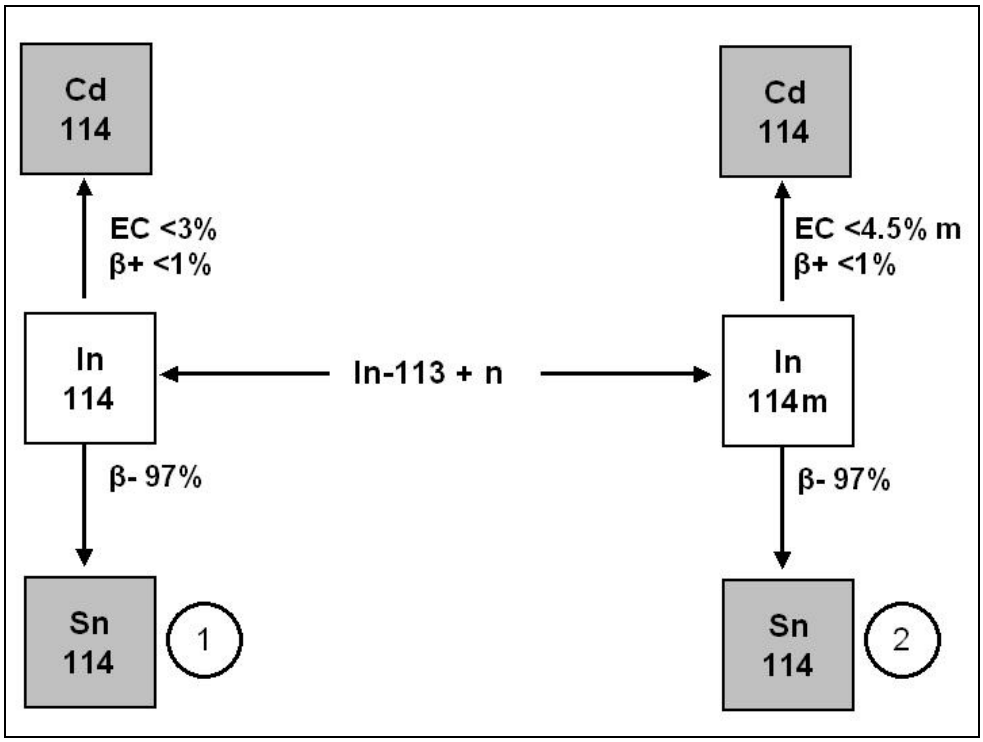

Figure 26 Decay Scheme for In-114 and In-114m

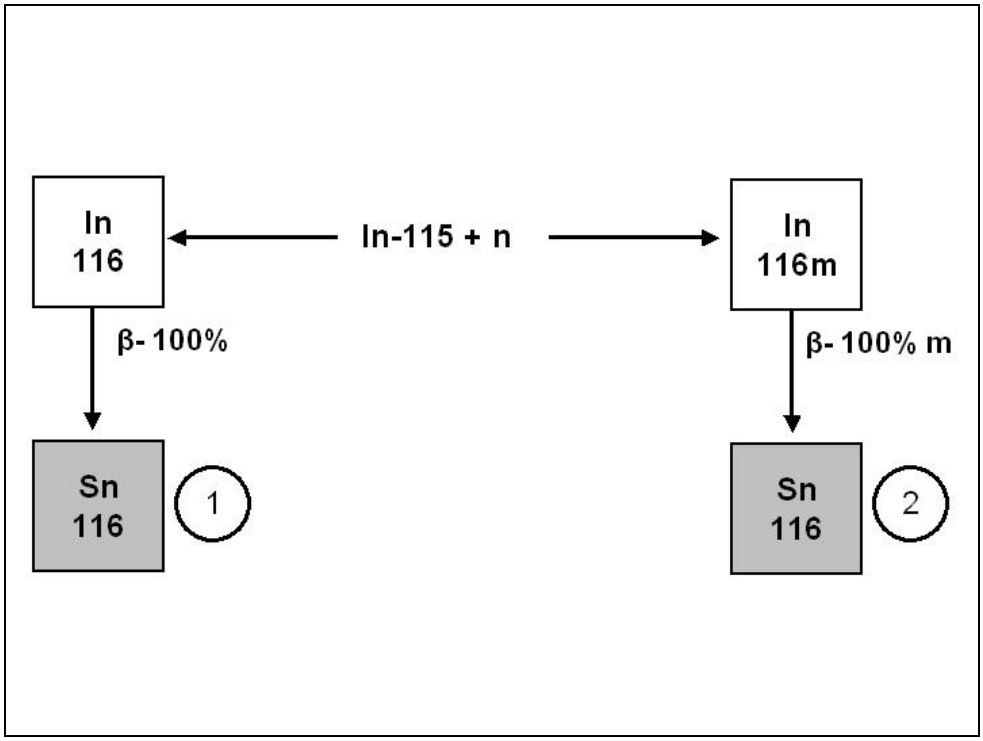

Figure 27 Decay Scheme for In-116 and In-116m

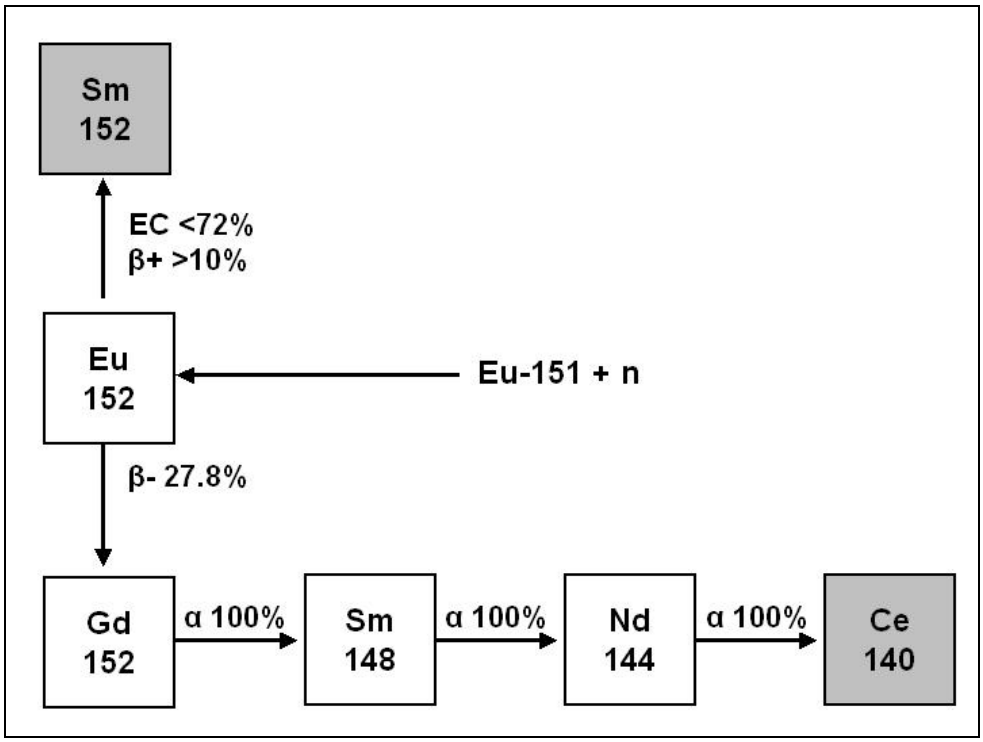

Figure 28 Decay Scheme for Eu-152

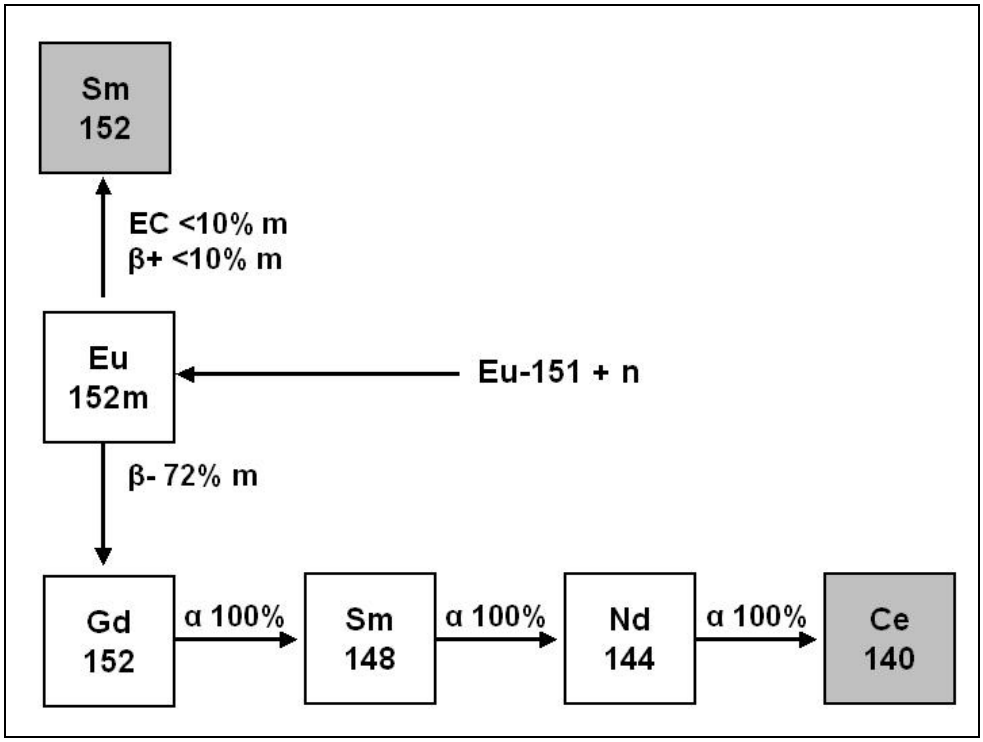

Figure 29 Decay Scheme for Eu-152m

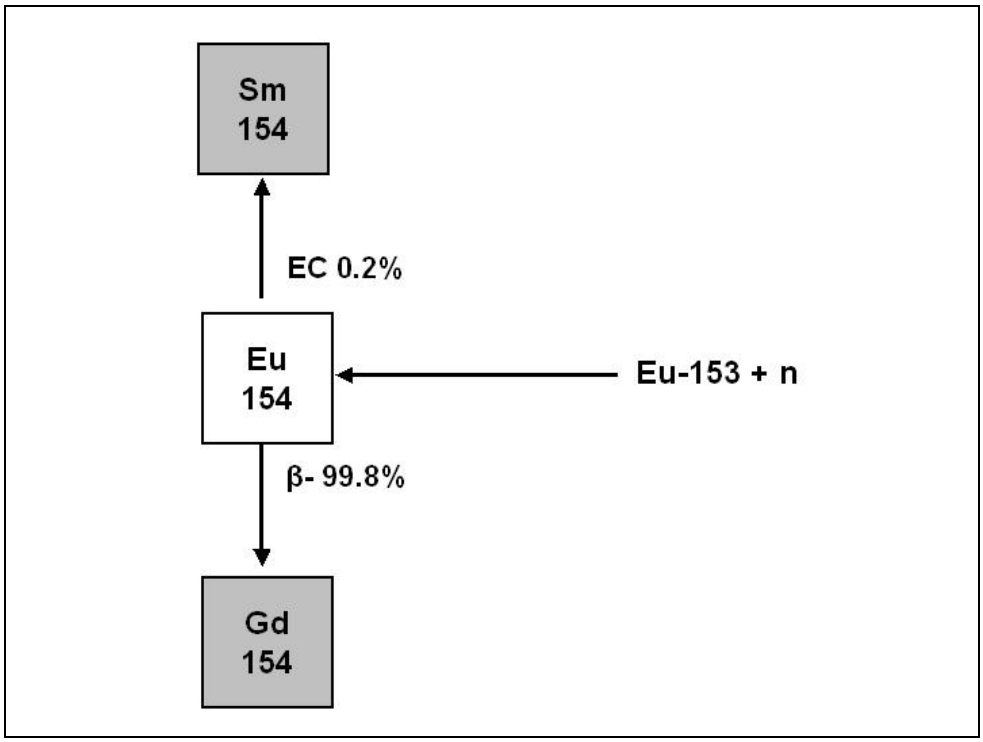

Figure 30 Decay Scheme for Eu-154

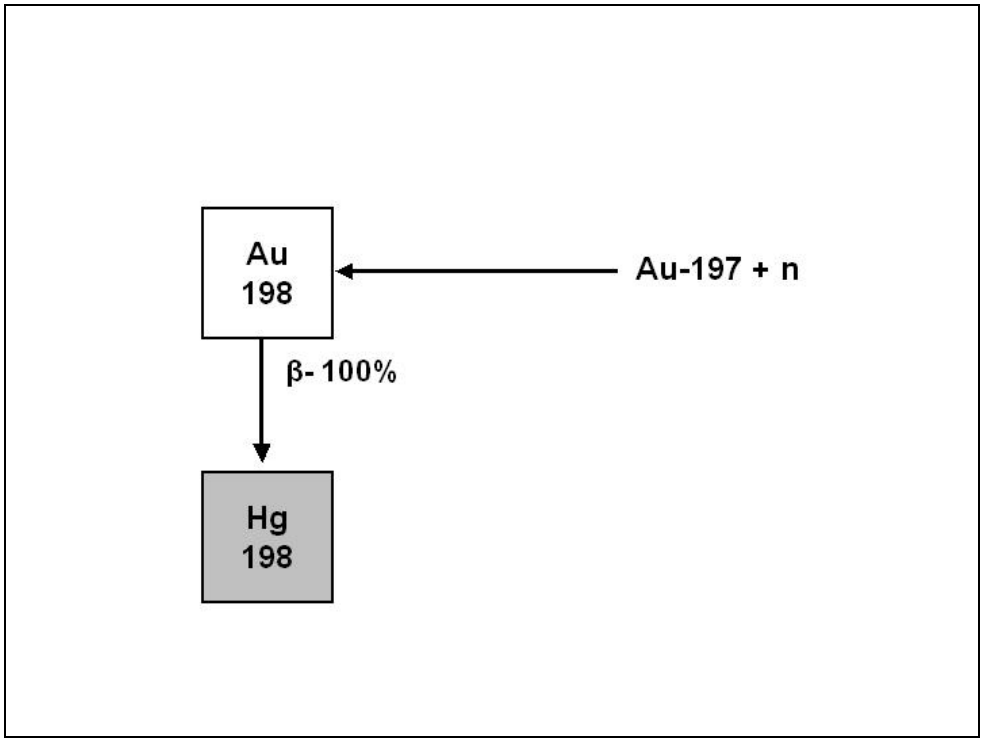

Figure 31 Decay Scheme for Au-198

Annex E. - HPGe Absolute Efficiencies Calculations

The HPGe intrinsic efficiency and the solid angle were combined to determine the absolute efficiency. These results are shown below.

Table 17 Absolute Efficiency

Key Gamma [keV]	HPGe Efficiency	Absolute Efficiency
97.43	0.034	3.672E-03
103.18	0.037	3.996E-03
121.78	0.046	4.968E-03
122.90	0.046	4.968E-03
190.27	0.055	5.940E-03
244.70	0.051	5.508E-03
344.27	0.042	4.536E-03
363.51	0.040	4.320E-03
411.79	0.037	3.996E-03
416.88	0.037	3.996E-03
433.92	0.036	3.888E-03
433.95	0.036	3.888E-03
558.43	0.030	3.240E-03
614.27	0.028	3.024E-03
618.85	0.028	3.024E-03
632.98	0.028	3.024E-03
657.74	0.027	2.916E-03
722.90	0.026	2.808E-03
723.31	0.026	2.808E-03
725.24	0.025	2.700E-03
763.93	0.025	2.700E-03
778.87	0.024	2.592E-03
841.54	0.023	2.484E-03
873.25	0.023	2.484E-03
884.67	0.023	2.484E-03
937.48	0.022	2.376E-03
963.34	0.022	2.376E-03
964.04	0.022	2.376E-03
996.37	0.021	2.268E-03
1004.87	0.021	2.268E-03
1085.83	0.020	2.160E-03
1097.23	0.020	2.160E-03
1112.09	0.020	2.160E-03
1274.50	0.019	2.052E-03
1293.49	0.018	1.944E-03
1384.27	0.018	1.944E-03
1408.02	0.017	1.836E-03

Bibliography

1) The White House Office of the Press Secretary *Text of Joint Declaration*. May 24, 2002.

2) The White House Office of the Press Secretary *Text of Strategic Offensive Reductions Treaty*. May 24, 2002.

3) Spears, David *Technology R&D for Arms Control*. US Department of Energy, National Security Administration, Defense Nuclear Nonproliferation Programs. Livermore, CA: Arms Control and Nonproliferation Technologies, Lawrence Livermore National Laboratory. Spring 2001.

4) Cartledge, Thomas E., Program Manager DTRA/Technology Applications Division "The Ideal Semiconductor Detector," Electronic Mail. 1155L. 12 August 2002.

5) ----. "Emerging Problems in Arms Control Technology." Electronic Briefing. 4 June 2002

6) Fetter, S., V.A. Frolov, M. Miller, R. Mozley, O.F. Prilutsky, S.N. Rodionov, and R.Z. Sagdeev, "Detecting Nuclear Warheads," in *Reversing the Arms Race: How to Achieve and Verify Deep Reductions in the Nuclear Arsenals*. Ed. F. von Hippel and R.Z. Sagdeev. New York: Gordon and Breach Science Publishers, 1990

7) Brigman, Charles J. *Introduction To The Physics of Nuclear Weapon Effects*. Fort Belvoir, Virginia. Defense Threat Reduction Agency. July 2001.

8) Knoll, Glenn F. *Radiation Detection and Measurement* (Third Edition). New York: John Wiley & Sons, Inc. 2000.

9) Turner, James E. *Atoms, Radiation, and Radiation Protection*. New York: John Wiley & Sons. 1995.

10) Gilbert, W. F. "Activation Cross Section," in *A Manual of Reactor Laboratory Experiments*. Illinois: Argonne National Laboratory. January 1965.

11) Tsoulfanidis, Nicholas. *Measurement and Detection of Radiation*. New York: McGraw-Hill Book Company. 1983.

12) Stanford, George S. and James H. Seckinger. *Thickness Corrections For Neutron-Activated Gold Foils*. Springfield, Virginia: Clearing House for Federal Scientific and Technical Information, National Bureau of Standards, U.S. Department of Commerce. February 1969.

13) T-2 Nuclear Information Service Los Alamos National Laboratory." Interpreted ENDF file for Cd-nat - capture cross section" n. pag. http://t2.lanl.gov/cgi-bin/endf?3,102,/inet/WWW/data/data/ENDF-neutron/Cd/nat. Accessed on 30 September 2002.

14) Canberra Industries, Inc. *Genie 2000 Spectroscopy System*. Meriden, Ct: Canberra Industries. 2001.

15) Ludlum Measurements, Inc. "Model 12-4 Neutron Meter" Product webpage. n. pag. http://www.ludlums.com/product/m12-4.htm. Accessed on 06 January 2003.

16) Constellation Technology Corporation. Contract DTRA01-99-C-0187 44-0088-01 with the Defense Threat Reduction Agency. Largo FL, 17 July 2002.

17) Kumar, Arun and P. S. Nagarajan. *Neutron Spectra of ^{239}Pu-Be Neuron Sources*. Nuclear Instruments and Methods. North-Holland Publishing Co. 140: 175-179. (1977).

18) Parrington, Josef R., Knox, Harold D., Breneman, Susan L., Baum, Edward M., and Feiner, Frank *Nuclides and Isotopes* (Fifteenth Edition). GE Nuclear Energy: Lockheed Martin. 1996.

19) Glascock, Michael D. *Neutron Activation Analysis Tables*. University of Missouri: Research Reactor Facility. July 1985.

20) Canberra Industries. Product webpage. n. pag. http://www.canberra.com/index2.htm. Accessed on 06 January 2003.

21) Monsanto Research Corporation. "Plutonium Neutron Source Shipping Documents for Neutron Source M-1170". Mound Laboratory: Miamisburg Ohio. March 9, 1962.

22) Christian, Gary D. *Analytical Chemistry* (Fifth Edition). New York: John Wiley & Sons. 1994.

23) Price, Jonathan B. Market Manager, Saint-Gobain, Newberry OH. Personal Correspondence. 3 January 2003.

24) Heath, R. L. *Gamma-Ray Spectrum Catalogue Ge(Li) and Si(Li) Spectrometry* (Third Edition - Volume 2 of 2). Springfield, Virginia: National Technical Information Service, US Department of Commerce. 1964.

Vita

Major Stephanie Vaughn was born in Englewood, Colorado. In 1987 she was awarded a Bachelor of Science degree in Microbiology from Colorado State University, Fort Collins, Colorado.

Major Vaughn received her commission into the United States Army as a Chemical Officer in January 1990 from Officer Candidate School, Fort Benning, Georgia. Her first assignment completing the Chemical Officer Basic Course was as the executive officer for Headquarters and Headquarters Company 3rd Corps Support Command in Wiesbaden, Germany. For the next five years Major Vaughn served in various positions across Europe including platoon leader for 95th Chemical Company, Vilseck, Germany and G3 operations officer for the Southern European Task Force, Vincenza, Italy. In February 1996 Major Vaughn attended the Chemical Officer Advanced Course and after graduation she was assigned to the 555th Engineer Group in Fort Lewis Washington. In August of 1998, Major Vaughn commanded Delta Company, 82nd Chemical Battalion, Fort McClellan, Alabama and in July 1999 moved the company to Fort Leonard Wood, Missouri. In August of 2001, she entered the School of Engineering, Air Force Institute of Technology.

REPORT DOCUMENTATION PAGE

Form Approved
OMB No. 074-0188

1. REPORT DATE *(DD-MM-YYYY)*	2. REPORT TYPE	3. DATES COVERED *(From – To)*
09-03-2003	**Master's Thesis**	Jun 2002 – Mar 2003

4. TITLE AND SUBTITLE

INVESTIGATION OF A PASSIVE, TEMPORAL, NEUTRON MONITORING SYSTEM THAT FUNCTIONS WITHIN THE CONFINES OF START I

5a. CONTRACT NUMBER

5b. GRANT NUMBER

5c. PROGRAM ELEMENT NUMBER

6. AUTHOR(S)

Vaughn, Stephanie, Major, USA

5d. PROJECT NUMBER

5e. TASK NUMBER

5f. WORK UNIT NUMBER

7. PERFORMING ORGANIZATION NAMES(S) AND ADDRESS(S)

Air Force Institute of Technology
Graduate School of Engineering and Management (AFIT/EN)
2950 P Street, Building 640
WPAFB OH 45433-7765

8. PERFORMING ORGANIZATION REPORT NUMBER

AFIT/GNE/ENP/03-10

9. SPONSORING/MONITORING AGENCY NAME(S) AND ADDRESS(ES)

DTRA/TDAS
Attn: MAJ Thomas Cartledge
8725 John J. Kingman Rd DSN: 221-9670
FT Belvoir, VA 22060-6201 e-mail: Thomas.Cartledge@DTRA.MIL

10. SPONSOR/MONITOR'S ACRONYM(S)

11. SPONSOR/MONITOR'S REPORT NUMBER(S)

12. DISTRIBUTION/AVAILABILITY STATEMENT

APPROVED FOR PUBLIC RELEASE; DISTRIBUTION UNLIMITED.

13. SUPPLEMENTARY NOTES

14. ABSTRACT

This study is an investigation of the theoretical and experimental possibilities of using activation foils to detect and monitor special nuclear material for treaty monitoring purposes. None of the experiments demonstrated sufficient sensitivity to detect the target flux of 0.5 neutrons/cm^2-sec. The target flux could be detectable, if the limit of detection had been reduced by a factor of 4 to 6. However, many issues identified could enhance the sensitivity including: increasing foil size, increasing detector efficiency, and optimizing foil selection.

The theoretical portion focused on gold, silver, indium, europium, and gadolinium foils and determined the minimum flux detectable, minimum time needed to detect a specific flux, and what gaps in coverage exist when a detection package consists of all combined foils. All calculations are based on actual gamma and beta detector responses and statistics in a high and low background.

The second section consists of experiments with gold, indium, and silver foils. Detectors in a low background counted emitted gammas or betas to establish three-sigma limits of detection, which is the lowest neutron flux detectable with a 99 percent statistical reliability. The dominant factor in determining the limit of detection is the error associated with the total activity. The determined value for limit of detection was used to calculate the minimum foil surface area required to detect the target flux.

15. SUBJECT TERMS

Foil Activation, Neutron Detection, Gold, Silver, Indium, Europium, Gadolinium

16. SECURITY CLASSIFICATION OF:			17. LIMITATION OF ABSTRACT	18. NUMBER OF PAGES	19a. NAME OF RESPONSIBLE PERSON
a. REPORT	b. ABSTRACT	c. THIS PAGE			James C Petrosky, LTC, USA (ENP)
U	U	U	UU	92	19b. TELEPHONE NUMBER *(Include area code)* (937) 255-6565, ext 4824; e-mail: jpetrosky@afit.edu